MODELING AND FAULT DETECTION OF AN INDUSTRIAL COPPER ELECTROWINNING PROCESS

by
SUSAN WIEBE

Thesis presented as a partial requirement in the
Master of Applied Science (M.A.Sc.)
in
Natural Resources Engineering

Faculty of Graduate Studies
Laurentian University
Sudbury, Ontario, Canada

THESIS DEFENCE COMMITTEE/COMITÉ DE SOUTENANCE DE THÈSE
Laurentian Université/Université Laurentienne
Faculty of Graduate Studies/Faculté des études supérieures

Title of Thesis
Titre de la thèse MODELING AND FAULT DETECTION OF AN INDUSTRIAL COPPER ELECTROWINNING PROCESS

Name of Candidate
Nom du candidat Wiebe, Susan

Degree
Diplôme Master of Applied Science

Department/Program
Département/Programme Natural Resources Engineering

Date of Defence July 24, 2015
Date de la soutenance

APPROVED/APPROUVÉ

Thesis Examiners/Examinateurs de thèse:

Dr. Helen Shang
(Supervisor/Directrice de thèse)

Dr. Turgut Yalcin
(Committee member/Membre du comité)

Dr. Eduard Guerra
(Committee member/Membre du comité)

Dr. Moshood Olanrewaju
(External Examiner/Examinateur externe)

Approved for the Faculty of Graduate Studies
Approuvé pour la Faculté des études supérieures
Dr. David Lesbarrères
Monsieur David Lesbarrères
Acting Dean, Faculty of Graduate Studies
Doyen intérimaire, Faculté des études supérieures

ACCESSIBILITY CLAUSE AND PERMISSION TO USE

AUTHOR'S DECLARATION

In presenting this thesis in partial fulfillment of the requirements for a Master of Applied Science degree at Laurentian University, I allow that the university's library shall make it freely available for reference and study. I further authorize Laurentian University to reproduce this dissertation by photocopying or by other means, in total or in part, at the request of other institutions or individuals for the purpose of scholarly research. It is understood that copying or publication of thesis for financial gain shall not be allowed without my written permission.

(Signature): _____

Department of Natural Resources Engineering

Laurentian University

Sudbury, ON, Canada

Abstract

Copper electrowinning plants are where high purity copper (Cu) product is obtained through electrochemical reduction of copper from the leaching solution. The presence selenium (Se) and tellurium (Te) in copper sulphide minerals may result in contamination of the leach solution and, eventually of the copper cathode. Unfortunately, hydrometallurgical processes are often difficult to monitor and control due to day-to-day fluctuations in the process as well as limitations in capturing the data at high frequencies. The purpose of this work is to model key variables in the copper electrowinning tank and to apply statistical fault detection to the selenium/tellurium removal and copper electrowinning process operations.

First principle modeling was applied to the copper electrowinning tank and partial differential equation models were derived to describe the process dynamics. Industrial data were used to estimate the model parameters and validate the resulting models. Comparison with industrial model shows that the models fit reasonably well with industrial operation. Simulations of the models were run to explore the dynamics under varying operating conditions. The derived models provide a useful tool for future process modification and control development.

Using the collected industrial operating data, dynamic principal component analysis (DPCA) based fault detection was applied to Se/Te removal and copper electrowinning processes at

Vale's Electrowinning Plant in Copper Cliff, ON. The fault detection results from the DPCA based approach were consistent with the industrial product quality test. After faults were detected, fault diagnosis was then applied to determine the causes of faults. The fault detection and diagnosis system helps define causes of upset conditions that lead to copper cathode contamination.

Acknowledgements

I am using this opportunity to express my gratitude to everyone who supported me throughout the course of this dissertation. I am thankful for your continuous guidance, constructive criticism and friendly advice during the project work.

Foremost, I would like to express gratitude to my advisor, Dr. Helen Shang from Laurentian University for her continuous support of my study and research. This work would not have been possible without your patience, constant motivation, guidance and immense knowledge.

I would also like to thank my external supervisors, Ms. Christiane Sgouros and Mr. Morris Wong from Vale's Copper Cliff Nickel Refinery – Electrowinning Process Technology group and all the people who provided me with the facilities and conducive conditions to complete this work. I am also sincerely grateful to you for sharing your views on a number of issues related to the project.

Last but not least I would like to thank my family: my husband Ryan St. Georges for your unconditional love, support and encouragement through many long hours and weekends, my parents Michael and Janet Wiebe for always being there for me and providing a keen interest in all that I do and finally to my sisters Laura, Heather and Patricia Wiebe for keeping me motivated.

Thanks for everything!

Susan Wiebe

Table of Contents

List of Figures

List of Tables

Chapter 1: **Introduction**

This introductory chapter outlines the motivation and objectives of this dissertation. A general outline and background information about the research topics and outline are also provided.

1.1 General Background

A major source of world copper production arises from copper-iron-sulphide minerals present in the earth's crust, such as chalcopyrite ($CuFeS_2$), bornite (Cu_5FeS_4) and chalcocite (Cu_2S) (Davenport, et al., 2002). To a lesser extent, oxidized copper minerals can also occur in forms of carbonates, hydroxyl-silicates and sulphates. The concentration or grade of copper in addition to the location and type of ore bodies present will often govern the mining method chosen to extract the valuable ore. Presence of high-grade nickel and copper sulphide ore deposits has made the Sudbury Basin (located in Ontario, Canada) one of the world's most renowned area for mining, mineral processing, smelting and refining of nickel and copper since the late 1800s. Today there are over a dozen mines in operation around the Sudbury Basin, mainly owned and operated by two large companies: Vale and Glencore.

The pyrometallurgical process, used in Sudbury and around the world, is more commonly used for copper extraction than hydrometallurgical methods. This is mainly due to the fact that Cu-Fe-S minerals are not easily dissolved by aqueous solutions. The pyrometallurgical process generally entails mining by means of surface or underground methods followed by

crushing and grinding to liberate the valuable minerals from the waste rock. The ore is subsequently processed by means of flotation to further separate and concentrate the minerals to a 30-35% copper grade (Khouraibchia, 2009). The resultant concentrate is then smelted and converted to form a 98.5% copper product known as “blister copper”. After some further pyrometallurgical treatment, the copper is casted into 99.5% pure copper anodes. The final refinement involves electrorefining the copper anodes to produce copper cathodes with 99.99% copper content. Alternatively in the case of low grade copper oxides and some copper sulphide minerals, it can be more economical to extract the copper by a fully hydrometallurgical process: leaching, solvent extraction followed by electrowinning to produce a copper metal of 99.99% purity.

1.1.1 Electrometallurgy

Electrometallurgy has a relatively short history in comparison to pyrometallurgy and hydrometallurgy since it was founded only after the discovery of electricity in the nineteenth century (Sany, 2009). Over the years, numerous advancements have been made to optimize electrometallurgical metal purification. Accordingly, more than 50 percent of copper today is purified by electrometallurgical processes instead of by a pyrometallurgical one.

Electrometallurgy can be subdivided into two main categories: electrorefining and electrowinning. In electrorefining, metal anodes are placed in a bath of acidic solution and the power supply causes the metal to dissolve and subsequently deposit on the cathode at a higher purity. Comparatively in the case of electrowinning, the metal of interest is added to

the electrolyte via mixing with a metal rich aqueous solution before electro-deposition on the cathode as pure metal.

1.1.2 Electrowinning of Copper

The electrowinning current is supplied through metallic conductors, two electrodes and the application of DC power (Sany, 2009). The electrochemical reactions occur at the electrolyte–electrode boundaries. Specifically in the instance of copper electrowinning, the copper is reduced and plated on the cathode electrode as per the reaction below:

$$Cu^{2+} + 2e^{-} \rightarrow Cu \qquad E^0 = 0.34V$$

At the same time, the oxidation reaction at the anode will cause oxygen to evolve:

$$H_2O \rightarrow 2H^{+} + \frac{1}{2}O_2 + 2e^{-} \qquad E^0 = 1.23V$$

Realized by Faraday's Law, the plating rate of metal *P* (g/s) strongly depends on the quantity of supplied electrical current *I*:

$$P = \frac{M_i \phi_i I}{Z_i F}$$

Accordingly, M_i is the molecular weight of species *i*, *I* is the total electric current applied to the cell, *F* is the Faraday's constant 96,500 Coulombs per equivalent mole, Z_i is the number of electrons involved in the reaction per number of metal ions plated and ϕ_i is the current efficiency of species *i*, in this case copper to deposit on cathodes.

Current efficiency, ϕ_i, provides a reasonable measurement of the cell's performance. It is calculated based on the difference between the weight obtained via Faraday's Law and the actual weight from the electrowinning process. A 100% current efficiency is unachievable in practice since there are other competing electrochemical reactions occurring that consume some of the electrical current. For example, ferric ions, commonly present in copper pregnant electrolyte, causes a loss of current efficiency. Ferric ions are continuously reduced to ferrous ions at the cathode and oxidized back to ferric ions at the anode:

$$Fe^{3+} + e^{-} \rightarrow Fe^{2+}$$

$$Fe^{2+} \rightarrow Fe^{3+} + e^{-}$$

Other factors besides current efficiency must be taken into consideration to optimize the metal deposition in terms of quantity and quality. The quality of the copper deposit may be affected by such influences as: current density, copper concentration, temperature and the presence of other impurities. For example, a coarse-grained deposit typically forms if the current density (amperage per square meter) is relatively low; a result of slow electrochemical reactions relative to the rate of surface diffusion of the copper ad atoms. In electrowinning, a relatively fine-grained deposit is favourable due to the smoother morphology of the copper plate. A coarse-grained deposit may also form with a higher metal ion concentration and/or higher electrolytic temperature and/or without the use of organic leveling agents. The concentration of other impurities, such as Se and Te, can also greatly affect the overall physical and/or chemical quality of the plated copper. Moreover, there are different grades of copper that must be below certain impurity concentrations in order to receive full value for the product.

1.1.3 Impurities - Selenium and Tellurium

Selenium (Se) and Tellurium (Te) are found in small concentrations under the earth surface yet have numerous applications, from improving machinability of ferritic steels to employment in the optoelectronic industry to glassmaking (Sany, 2009). Typically, Se and Te coexists with pyritic sulphide minerals such as pentlandite ($(FeNi)_9S_8$), chalcopyrite ($CuFeS_2$), pyrite (FeS_2), sphalerite (ZnS) and pyrrhotite ($Fe_{(1-x)}S$ (x = 0 to 0.2)). There are, however, no specific deposits for Se and Te but rather they are recovered as a by-product of other metal processing streams. These elements are associated most commonly with the recycling of anode slimes; the accumulation of solids at the bottom of copper electrorefining or electrowinning cells. A treatment process involving a reductant such as SO_2 gas or copper metal is then required to precipitate the Se and Te when reprocessing the anode slimes or high Se/Te streams. Otherwise, Se and Te will most likely plate with the copper beyond the assigned grade specifications and render the product unsalable or require a lot of process rework at significant cost and market delay. Other base metal (i.e., Fe, Ni, Zn) are also capable of further reducing elemental Se and Te to different forms but this can introduce new impurities to the electrolyte (Mokmeli, et al., 2014). Hence, utilizing copper metal is preferable to remove the Se and Te impurities as it does not further contaminate the copper electrolyte solution.

1.2 Motivation

The general purpose of Vale's Copper Cliff Electrowinning Plant is to produce high purity copper product. The electrowinning process is the final and critical step in producing the copper cathode. Modeling the electrowinning process has been studied by researchers from academia and industrial practitioners. Existing models have been focused on steady state models without considering variable variations with time. Available steady state models provide a useful foundation for process design. Dynamic modeling incorporating variable variations may be useful for process control. Dynamic modeling for the copper electrowinning process is explored in this thesis. The process dynamics and the effects of operating conditions are studied based on the developed models.

The final purification step of copper electrowinning electrolyte involves a Se and Te removal process. Unfortunately, the chemistry of the process is poorly understood, making it difficult to pinpoint causes when issues arise. The presence of Se and Te in the solution can seriously jeopardize the quality of copper product. Application of statistical approaches to process data has been recognized as a powerful tool in processing large amount of process data and addressing process monitoring and diagnosis problems. Among the statistical approaches, principle component analysis (PCA) has been extensively applied in a wide range of processes and subjects. In this thesis, a fault detection method using dynamic principal component analysis (DPCA) was applied to the Se/Te removal and copper electrowinning processes. In such processes systems, time lag and significant residences times exist and therefore should be accounted for when predicting faults in data. DPCA uses time lagged

information to acquire more reliable detection. This contribution is expected to provide a better understanding and control of impurity removal and tankhouse operations.

Chapter 2: **Literature Review**

This section provides an overview of past literature and research relating to the removal of selenium/tellurium impurities and the modeling of the copper electrowinning process.

2.1 Se/Te Removal

Although selenium and tellurium minerals may represent an insignificant portion of most sulphide ores, their concentrations can increase to a point of exceeding contamination limits for the pregnant electrolyte after several metallurgical treatments (Mokmeli, et al., 2014). To avoid contamination of the final electrowon product, the selenium and tellurium must be removed from solution prior to electrowinning by treating the solution with a reducing agent such as SO_2 gas or less noble metal. However, most research around selenium and tellerium removal is on the topic of treating copper anode slimes as a byproduct from copper refineries and not from the feed stream to an electrowinning process. Anode slimes, containing upwards of 28% Se and 8% Te, represents the main source for most of world's production of selenium and tellurium (Rao, et al., 1976).

At Phelps Dodge's refinery in El Paso the Te-Se enriched leached solution is treated by cementation in a copper chip tower at 93^oC for 24 hours. Effectively, precipitates of copper

selenides and tellurides are formed and filtered from solution according to the following overall reactions:

$$H_2SeO_3 + 4Cu + 2H_2SO_4 \rightarrow Cu_2Se + 2CuSO_4 + 3H_2O$$

$$H_2TeO_3 + 4Cu + 2H_2SO_4 \rightarrow Cu_2Te + 2CuSO_4 + 3H_2O$$

Today there are several examples of industrial plants that utilize copper metal as a means to reduce Se and Te from an acidic copper sulphate solution. Some other examples include Naoshima's refinery in Kagawa, Japan and Vale's Electrowinning Plant in Copper Cliff, ON, Canada (Mokmeli, et al., 2014).

Recent work at the University of British Columbia (Mokmeli, et al., 2014) has enhanced the understanding of selenium and tellurium removal using a copper metal. A noted finding was that the reduction of Se^{VI} and Te^{VI} is a result of reaction with cuprous ion and not the surface reaction with the copper metal itself. In order to have efficient removal of Se and Te, therefore, the cuprous concentration must be preserved by minimizing its oxidation by reaction with ferric ions:

$$Cu^{+} + Fe^{3+} \rightarrow Cu^{2+} + Fe^{2+}$$

This is done by reducing ingress of oxygen to the reaction site, maintaining temperature close to boiling point and high acidity.

A different approach to modeling the effects of selenium and tellurium removal is utilized in this work. The first principles model that uses differential equations (Mokmeli, et al., 2014) is converted to a discrete model so that it can be conveniently fit with industrial operating data. The resulting model can be used to predict dynamic variation of output and/or provide an online estimate for variables that are measured infrequently. Rather than using rate reduction laws, data driven models are applied.

2.2 Copper Electrowinning

Electrorefining of copper is one of the oldest industrial electrolytic processes and one of the most common electrowon metals. As such, there are a plethora of studies surrounding the subject of copper electrodeposition. Although technological advancements have improved the understanding and operation of the process, the basic principles and main equipment are still as applicable today as they were over a century ago (Beukes & Badenhorst, 2009).

Aminian et al. uses process modeling to predict the influence of variables such as copper concentration and cell voltage on the current efficiency and performance of the process (Aminian, et al., 2000). In this case, process models were developed from first principles for both solvent extraction (SX) and electrowinning (EW) processes and subsequently linked together as one unique simulator. The simulator was established to replicate and compare results from the SX/EW circuit of Gaspé mines. Aminian et al. concludes that despite numerous assumptions made during the development of the simulator, the simulated results agreed closely with the actual data.

Similarly, Lie et al. decided to model the copper process at Xstrata Nikkelverk Refinery (Kristiansand, Norway) including the copper leaching and electrowinning process (Lie & Hauge, n.d.). Due to time delays, multivariable behavior and nonlinearities in the process, a model based control was necessary to try and improve variation in quality. Accordingly, a dynamic model with 39 variables was formulated from steady state total mass balances, reaction kinetics as well as steady state and dynamic species balances. The model was further simplified by incorporating known process data from available industrial measurements. The remaining unknown parameters such as current efficiency and steady states were solved for via linear equations by means of the least squares method.

Chapter 3: **Technical Background**

This chapter briefly discusses and defines the technical terms utilized in this dissertation.

3.1 Dynamic Modeling & Process Monitoring

A process model is an equation or set of equations that possesses a predictive quality about the process. Process models can be useful in not only improving the understanding of the process but also in developing a control strategy of a new process as well as to optimize process operating conditions(Seborg, et al., 2004). First principle (also known as theoretical models) models as the name implies utilizes strictly fundamentals derived from engineering, chemistry or physics to create reasonable representation of the process. Conversely, empirical models are stringently data driven by fitting experimental data. In industry fundamental equations and experimental data are generally preferred to come up with the best process model. One or more of the parameters from the theoretical model are then calculated from experimental data instead of assumed.

Dynamic models take into account the behaviour over time by applying unsteady state conservation laws. Generally, dynamic models of a chemical process can be represented as an Ordinary Differential equation (ODE) or a combination of Partial Differential Equations (PDE) and algebraic equations. Algebraic equations involve relationships progressed from

thermodynamics, transport phenomena, chemical kinetics, etc. The resulting model can then be used to predict dynamic variation of output.

The principal objective of process control is to sustain a process at the desired operating conditions while ensuring safety, the environment, efficiency and product quality are not compromised (Seborg, et al., 2004). In order to ensure that the process is maintained, the process should be monitored for excursions or for abnormal behaviour using process monitoring techniques. There are three main steps in process monitoring: routine monitoring, detection and diagnosis and preventive monitoring. Routine monitoring is the simple task of looking to see if the process variables fall in or out of specified operating control limits. Step two is commenced by the detection of an abnormal process upset that is then investigated for causes and diagnosed. Finally, preventive monitoring, through corrective action, prevents the upset from seriously affecting the process.

Process monitoring employs process data and statistically-based techniques, known as statistical process control (SPC), to improve process performance and product quality. Strictly, data driven approaches derived from process data are generally not ideal due to the sheer volume of data that can be available from a modern industrial process. It is difficult or cumbersome for an operator or engineer to properly analyze the process by merely observing enormous amounts of data. For example, Limit Checking is a traditional SPC monitoring approach to detect if the process measurements are within specified upper or lower control limits and to restrict rate of change or for sample variance. Although, all processes inevitably

contain some variability, it is important to note the difference between normal and abnormal variability. Normal variability, also known as random variability, is essentially noise or turbulence that could not have been controlled or eliminated (chance cause). Abnormal variability is non-random and caused by instrumentation malfunctions, process changes, human error or other assignable causes that could have been avoidable. In order to determine if the process operation is normal or abnormal, the SPC monitoring techniques are used in conjunction with control charts.

The traditional SPC monitoring technique is often constrained by its univariate approach; where one process variable is controlled and one variable is manipulated. This traditional statistical technique is therefore not suitable for an industrial process that has multiple process variables. A multivariable process requires multivariate statistical techniques, such as Principal Component Analysis (PCA) to better predict normal and abnormal behavior.

3.2 Fault and Fault Detection

With the increasing demands for higher system performance, product quality and cost efficiency, one of the most critical issues surrounding the design of automatic systems is the system reliability and dependability. A traditional way to improve the system reliability and dependability is to enhance the quality, reliability and robustness of individual system components like sensors, actuators, controllers or computers. Even so, a fault-free system operation cannot be guaranteed. Process monitoring and fault diagnosis are becoming an ingredient of a modern automatic control system (Ding, 2013).

The term fault is generally defined as a departure from an acceptable range of an observed variable or a calculated parameter associated with a process (Himmelblau, 1978) . Fault detection and diagnosis deals with the timely detection, diagnosis and correction of abnormal conditions of faults in a process. Early detection and diagnosis of process faults while the plant is still operating in a controllable region can help avoid abnormal event progression and reduce productivity loss. Since the petrochemical industries lose an estimated 20 billion dollars every year, they have rated Abnormal Event Management (AEM), of which fault detection and diagnosis is the central component, as their number one problem that needs to be solved (Nimmo, 1995). Hence, there is considerable interest in this field now from industrial practitioners as well as academic researchers.

3.3 Principal Component Analysis (PCA)

Principal Component Analysis (PCA) is a useful technique for analyzing and monitoring data. The main advantage of PCA is its ability to reduce the dimensionality of the data without losing significant information. This is established by creating new variables called principal components, which are a smaller set of variables that contain the most of information of the original data set such as variance. The importance of the each principal component (PC) is then categorized by the fraction of information each retains. This technique is also known as image compression (Smith, 2002).

The Principal Component Analysis (PCA) is carried out in five steps: Centering, Covariance Matrix, Eigenvectors and Eigenvalues, Component Selection and New Data Set. The first step in PCA is centering of the data set, by subtracting the mean of the data from each data point. For instance, consider a vector ***x*** with an ***m*** number of variables that have been adjusted to unit variance. The purpose is to normalize the data and construct a data set with a mean of zero.

The second step is to calculate a covariance matrix. Covariance is calculated when there is more than one dimension, to determine the variance with respect to each dimension. Let ***S*** represent the covariance matrix of ***x*** as follows:

$$S = \frac{x^T x}{(m-1)}$$

For example, if there are 3 dimensions (x, y, z) then the covariance is measured between x and y, y and z and, z and x. This example would then produce a respective covariance matrix, *S*:

$$S = \begin{bmatrix} \mathrm{cov}(x,x) & \mathrm{cov}(x,y) & \mathrm{cov}(x,z) \\ \mathrm{cov}(y,x) & \mathrm{cov}(y,y) & \mathrm{cov}(y,z) \\ \mathrm{cov}(z,x) & \mathrm{cov}(z,y) & \mathrm{cov}(z,z) \end{bmatrix}$$

Consequently, if the covariance is positive, the two respective dimensions would increase together, otherwise, if the covariance is negative, one dimension decreases as the other increases. The third step of the PCA method is to calculate the eigenvectors and eigenvalues of the covariance matrix. The number of eigenvectors is equivalent to the dimension of the covariance matrix (3 eigenvectors for the example above) and all eigenvectors are

orthogonal. Eigenvectors provide information about the pattern in the data, thereby expressing the data in terms of orthogonal eigenvectors, instead of in terms of x and y axes, reducing the dimensionality of the data. The data is then transformed in terms of these eigenvectors and the principal components are chosen. The principal component(s) is the eigenvector that best fits or explains the pattern in the data. In this case, the principal component is the eigenvector with the largest eigenvalue (>1), since it accounts for more variance than one of the original variables. Let p_k represent the eigenvector of S with the k^{th} largest eigenvalue λ_k:

$$t_k = p_k^T x$$

Moreover, ordering the eigenvalues will determine which eigenvectors (components) are significant to the data or not. The variation between t_k (the k^{th} principal component) and λ_k can be calculated as follows:

$$\%variation\ in\ t_k = \frac{\lambda_k}{\sum_k \lambda_k}\ (100) = \frac{\lambda_k}{trace(S)}(100)$$

If an eigenvalue is small and the corresponding eigenvector disregarded, the final data set will have less dimensions. The remaining principal components are combined to form a feature matrix.

The fifth and final step in PCA takes the transpose of this feature matrix and multiplies it on the left hand side of the transpose of the original centered matrix formed in step one. The transpose puts the eigenvectors in rows instead of columns for the feature matrix and the data

dimensions into rows instead of columns for the original data matrix. This final step allows the data to be expressed in terms of principal components instead of x and y axes, where *e* is the residual matrix:

$$x = t_1 p_1^T + t_2 p_2^T + \cdots + t_k p_k^T + e$$

A Principal Component Regression (PCR) can be formed by using the principal components of X or the "feature matrix" as the independent variables of a multiple linear regression model predicting Y. However, the main problem with this method is that PCA finds principal components that best explain X without optimally predicting Y.

Dynamic Principal Component Analysis (DPCA) takes PCA one step further by including a time lag to extract desired information from the process. For any chemical process, there are typically a large number of variables as well as large time lag between variables, making system diagnosis cumbersome. Similarly to PCA, DPCA will extract the data at reduced dimensions and apply the same strategy in forming time-lagged matrices.

Chapter 4: **Process Description**

For over a century, the presence of high-grade nickel and copper ore deposits has made the Sudbury Basin a prominent area for mining (Donald & Scholey, 2005). As the processing of ore has changed and advanced over the years, the resultant operations today has become one of the most complex mining operations in the world. Two large companies, Vale and Glencore, as well as a few smaller mining companies reside in Sudbury Basin with over a dozen mines in operation. The purpose of this chapter is to briefly review Vale's operations in Sudbury, Ontario with a more specific focus on the Copper Electrowinning Plant. Figure 1 displays the flow sheet for Vale Sudbury operations.

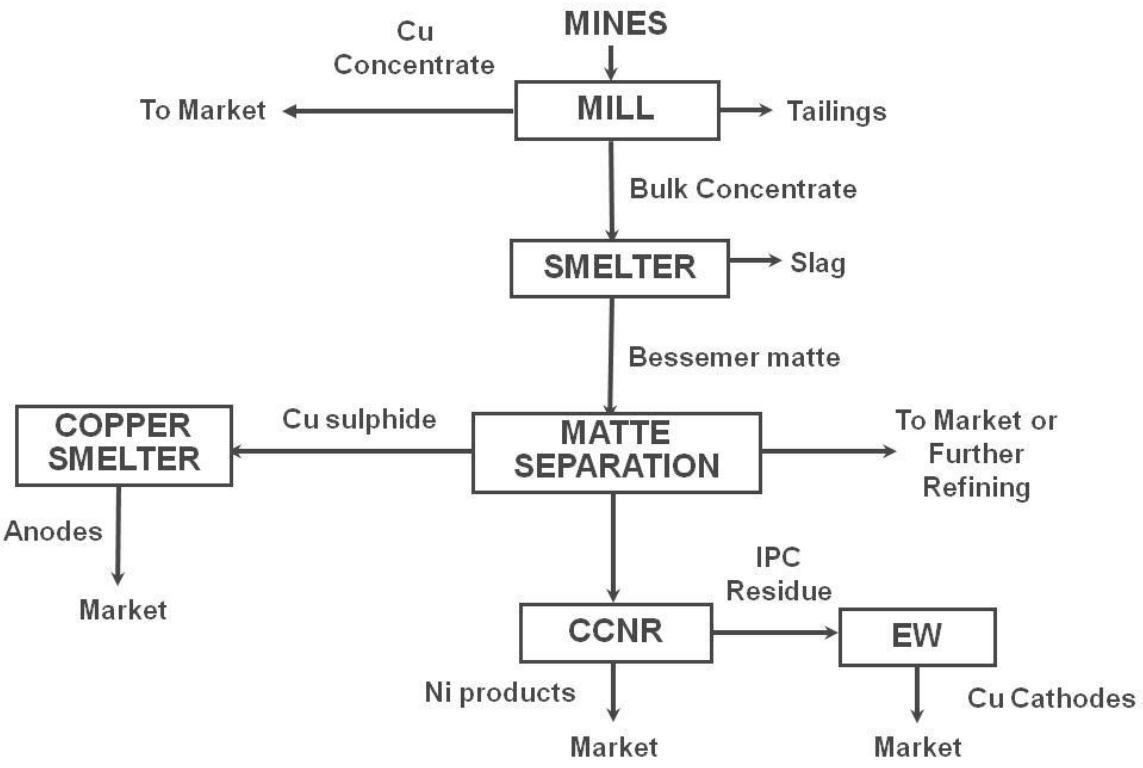

Figure 1: Vale's Sudbury operation flowsheet

Ore mined solely for Vale's operation include: Coleman Mine, Stobie Mine, Copper Cliff Mine, Creighton Mine, Totten Mine, Vale open pits and supplemented ore from third parties such as McCreedy West. Typical operating depths for Sudbury Basin underground mining range from 3000 to 6000 ft. However, if deposits extend deeper underground, such as the case with Creighton Mine, mining depths can be extended past 9000 ft. The actual mining methods vary significantly between mines and in the mine itself, depending on the ground conditions, geometry of the ore deposits, infrastructure, etc. The ore specifically for Vale's operation is properly crushed before subsequent processing at the Clarabelle Mill.

At the Clarabelle Mill, the majority of the ore is fed to a Semi Autogenous Grinding (SAG) mill followed by ball mills to ensure the ore is ground and liberated to the appropriate size. The ensuing concentration steps involve magnetic separation to remove pyrrhotite and flotation to form nickel bulk concentrate. This nickel bulk concentrate incorporates as the main feed to the smelting operation.

Approximately 3600 mtpd of nickel bulk concentrate is processed in the Clarabelle Mill and pumped to the smelter. The smelter’s filter plant reduces the moisture content in the nickel bulk concentrate to ~12%H_2O (Carr, et al., 1997). In addition, sand flux, mixed revert material and recycled flash furnace slimes are blended together with the bulk concentrate to produce a design of 4800 mtpd of feed for the furnaces.

The feed is first fluidized with air in a fluid bed dryer to further reduce the moisture to ~0.2% H_2O and then fed into the furnace. The dry feed is injected with oxygen into the furnace via four burners, two per end wall. Feeding the furnace with oxygen allows for the dry feed, a sulphide concentrate, to burn off some of its sulphur and iron and hence, "flash" smelted upon entry into the furnace. The sulphur dioxide (SO_2) enriched off-gas is captured through the center uptake and subjected to a gas cleaning process. Subsequently, gas cleaning cools and cleans the gas prior to recovery at the Acid Plant and Liquid SO_2 Plant.

In the furnace, the desired matte grade of 47% CuNiCo is mainly achieved by controlling the rate of oxygen flow through the burners and by supplementing the heat balance with natural gas and/or coke addition. The iron oxide and silica flux that make-up the slag layer is skimmed through the north end wall and transferred to the slag disposal site by rail-mounted slag pots. The heavier molten sulphides (matte), which contains the desired metals, is tapped into ladles from any four tap holes and charged into the Pierce-Smith converters. In the converters, oxygen is added through the tuyere line to react with the remaining iron and sulphur in the matte to produce slag and SO_2 off-gas (Donald & Scholey, 2005). Throughout the converting cycle, the slag is skimmed and returned to the flash furnaces for recovery of any desired metals (Cu, Ni, Co). Once the iron content in the matte is <0.8% and sulphur deficient, the matte, which is now considered Bessemer matte at ~ 75% matte grade (CuNiCo), is ready for casting. The ladles of Bessemer matte are poured into cast moulds and cooled for several days to form 25 ton ingots. The ingots are crushed, ground and classified to prepare for further processing.

The liberated minerals as a result of the Bessemer matte crushing and grinding are subsequently separated by means of magnetic separation. Magnetic separation allows the metallic Cu and Ni to be separated from the non-metallic fractions. Flotation is applied to the non-metallic fraction to effectively separate copper sulphide from the nickel sulphide. The copper sulphide portion moves forward to the smelter to form a blister copper and the nickel sulphide portion is roasted in a fluid bed roaster to form a nickel oxide. The resultant nickel oxide products are either sold to market or sent for further refining.

The first step in the refining of nickel involves reducing the nickel oxide feed to a metallic nickel. This is accomplished in a Top Blown Rotary Converter (TBRC), where the feed is subjected to high temperatures and coke addition to effectively melt and reduce to a metallic form, respectively. In the process, sulphur is oxidized to target a matte with a 3.5-4.0 Cu:S ratio. The resultant product is then granulated, decanted and dried before entering the Inco Pressure Carbonyl (IPC) reactor. The IPC reactor is essentially a high pressure (1000 psi) and high temperature ($180^{o}C$) vessel that utilizes carbonyl technology to extract nickel. The following reaction demonstrates the reaction between nickel and carbon monoxide gas:

$$Ni_{(s)} + 4\ CO_{(g)} \rightarrow Ni(CO)_{4(g)}$$

As the nickel is extracted at efficiency typically upwards of 97%, it is separated from the other remaining impurities such as copper, cobalt, iron, precious metals, etc. The resultant crude nickel liquid is then fed to a distillation column to preferentially distill the nickel

carbonyl and transport it to the decomposers. Predominantly, the pure nickel carbonyl is directly fed to one of seventeen pellet decomposers to produce nickel pellets. Although a portion of the carbonyl may be condensed and re-vapourized to a higher strength to produce a nickel powder product via powder decomposers. Finally, the IPC reactor residue, containing the bulk of the remaining impurities, is ground by a ball mill to produce suitable sizing for settling and separation at Vale's Copper Cliff electrowinning plant.

4.1 Electrowinning Plant

The plant encompasses several stages to recover copper and other valuable metals, nickel, cobalt and precious group metals, and to separate out further impurities such as iron and arsenic. Figure 2 below provides a basic block diagram of the Electrowinning Flow sheet, highlighting the main stages and process streams. This section briefly describes each step of Vale’s electrowinning plant with a focus on the Se/Te Removal and Electrowinning Circuits. (Vale Canada Ltd, 2014)

ELECTROWINNING

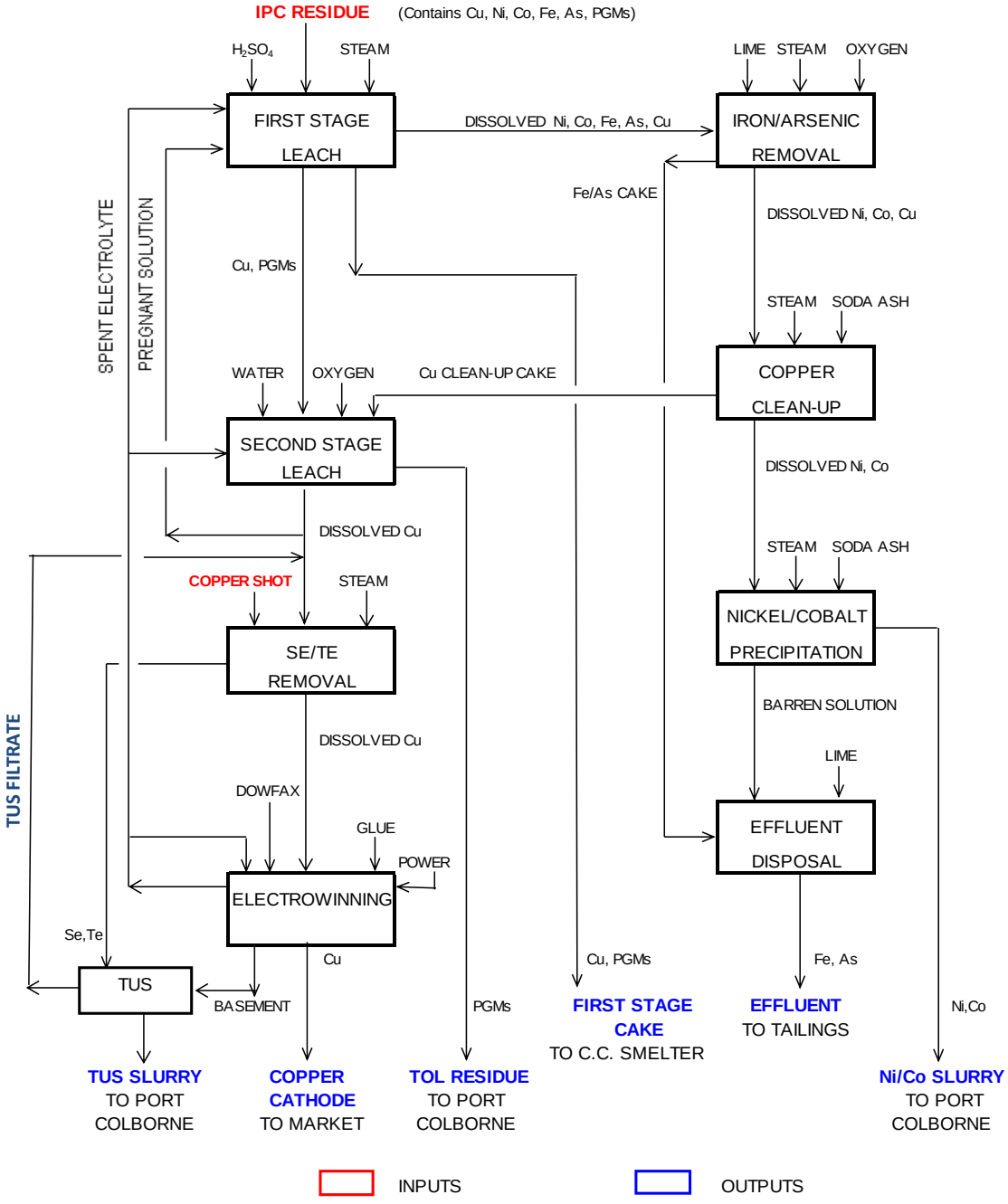

Figure 2: Diagram of Vale's copper electrowinning plant

First Stage Leach

The feed to the Electrowinning plant is a residue (IPC Residue) produced as a result of the pressure carbonylation process at the Copper Cliff Nickel Refinery. The residue has high concentrations of Cu and an assortment of other metals: Ni, Co, PGMs, Fe, As. Approximately 55 metric tonnes of residue is received into the plant per day and appropriately thickened from 10% to 55% solids. As the name implies, the 1st Stage Leach Circuit is the first leaching stage with the purpose of dissolving nickel (Ni), cobalt (Co), iron (Fe) and arsenic (As) back into solution. This leaching is achieved via sulphate pressure leaching in batch autoclaves @ 150^{o}C and 4.5 kg/cm^{2} pressure. The reaction takes about 1 hour followed by filtration to separate the leach solution from the remaining solids. This solution, also known as 1st Stage Filtrate, is then further treated in the Iron/Arsenic Removal Circuit.

Iron/Arsenic Removal

The Iron/Arsenic Removal Circuit essentially removes Fe and As from the 1st Stage Filtrate by means of precipitation with lime and oxygen. In a set of autoclaves, lime slurry is added to appropriately adjust the pH under oxygen pressure at 3 kg/cm^{2}. The resultant Fe and As is precipitated as ferric hydroxide and ferric arsenate, respectively. In order to recover the co-precipitated Ni and Co, the solids are subsequently repulped in acid to selectively re-dissolve most of the Ni and Co back into solution. After a set of filtration and water repulp stages, a final cake containing mainly Fe and As is directed to the Effluent Handling System, where the filtrate is pumped to the Cu Clean-Up and Ni/Co Recovery Circuit for further processing.

Copper Clean-Up and Nickel/Cobalt Precipitation

The Ni/Co Removal Circuit has two main purposes: first to recover any remaining Cu to the 2nd Stage Leach and secondly, to produce a concentrated Ni & Co carbonate slurry for further processing. During the first step, the pH of the Iron Filtrate is adjusted to 5.1 by means of adding soda ash (Na_2CO_3). This pH selectively precipitates the Cu as a carbonate but leaves Ni and Co in solution.

$$2CuSO_4 + 2Na_2CO_3 + H_2O \rightarrow CuCO_3 \cdot Cu(OH)_2 + 2Na_2SO_4 + CO_2$$

The slurry is subsequently thickened in a thickener to separate the Ni/Co enriched solution from the Cu solids. The Cu slurry is filtered via a drum filter to remove any entrained Ni/Co solution and produces a Cu Cake for recycle to the 2nd Stage Leach circuit. At this point, the Ni/Co enriched solution moves forward to the second step, known as the Ni/Co Precipitation Circuit. The pH is further adjusted with soda ash, 7 to 7.6 range, to favorably precipitate nickel and cobalt.

$$5NiSO_4 + 5Na_2CO_3 + 7H_2O \rightarrow 2NiCO_3.3Ni(OH)_2.4H_2O + 5Na_2SO_4 + 3CO_2$$

$$3CoSO_4 + 3Na_2CO_3 + 2H_2O \rightarrow 2CoCO_3.Co(OH)_2.H_2O + 3Na_2SO_4 + CO_2$$

The remaining solution that is barren is separated from the Ni/Co solids in a thickener and pumped to the electrowinning pond as effluent. However, the final Ni/Co is slurried with

water and effectively stored until trucks arrive to move the slurry for supplementary processing in Port Colborne, ON.

Second Stage Leach

The cake produced from 1st Stage Leach, containing significant portions of Cu and PGMs, Se and Te, is subjected to a second round of leaching. This Second Stage Leach process essentially leaches the Cu, Se and Te by means of sulphate oxidative pressure leaching and leaves the precious metals in solid form. Sulphate oxidative pressure leaching is carried out by mixing the first stage cake with spent electrolyte (sulphate) and by subsequently heating and pressurizing to 115^{o}C and 12 kg/cm^{2}, respectively. On a batch basis, the reaction can take up to 8 hours in a set of autoclaves. The following reactions displays how copper is leached from the Cu_2S or CuS form to a $CuSO_4$ soluble form:

$$2Cu_2S + 2H_2SO_4 + O_2 \rightarrow 2CuS + 2CuSO_4 + 2H_2O$$

$$2Cu_2S + CuSO_4 + O_2 + 2H_2O \rightarrow 2CuS + (2Cu(OH)_2.CuSO_4)$$

$$CuS + 2O_2 \rightarrow CuSO_4$$

The solid and solution are then separated in a set of filter presses. The concentrated precious metal press cake, also known as Total Oxidative Leach (TOL) residue, is repulped with water and stored and shipped to Port Colborne's Precious Metals Refinery on a weekly basis. Consequently, Second Stage Leach effectively leaches out more than 99% of Cu, which is

directed to the filtrate. This filtrate is now pregnant with Cu but requires another purification step to remove remaining impurities, mainly Se and Te.

Se/Te Removal

This stage effectively removes Se, Te and any remaining PGMs out of solution by means of cementation and settling. The pregnant electrolyte, containing up to 80 ppm Se and 80 ppm Te, is heated to 100^{o}C and pumped through a bed of copper shot at approximately 400 L/min.

Figure 3: Cu shot addition to column

The figure above demonstrates how the copper shot is added to the Cu Shot Column to maintain sufficient bed level. Essentially, the copper shot is conveyed over from a hopper to the top of the Cu Shot Column by means of a screw conveyor.

Under the right conditions, exposing the solution to this fine copper metal initiates the cementation reaction and causes the Se and Te to be reduced and precipitate as solids. In the process, the ORP of the solution changes from approximately 400 mV to 140-160 mV.

The following reactions exemplify that Te is precipitated in the Cu Shot Column as pure Te and various forms of copper telluride (Se follows the same reactions):

$$H_2TeO_3 + 2Cu + 4H^+ \rightarrow Te + 2Cu^{2+} + 3H_2O$$

$$H_2TeO_3 + 3Cu + 4H^+ \rightarrow CuTe + 2Cu^{2+} + 3H_2O$$

$$H_2TeO_3 + 4Cu + 4H^+ \rightarrow Cu_2Te + 2Cu^{2+} + 3H_2O$$

At this point, the removal of Se and Te from solution down to tolerable levels is unobtainable due to the presence of both 4+ and 6+ valence forms. Hence, the solution is subsequently aged in plug flow aging towers to allow enough time to complete the higher valence reactions. There are typically 12 to 14 hours of residence time provided, from the first aging tower to the final fourth aging tower. Therefore, Te^{6+} continues to be reduced and precipitates in the aging towers by the following reactions (Se follows the same reactions):

$$H_2TeO_4 + 3Cu + 6H^+ \rightarrow Te + 3Cu^{2+} + 4H_2O$$

$$H_2TeO_4 + 4Cu + 6H^+ \rightarrow CuTe + 3Cu^{2+} + 4H_2O$$

$$H_2TeO_4 + 5Cu + 6H^+ \rightarrow Cu_2Te + 3Cu^{2+} + 4H_2O$$

Resultantly, the concentrations of Se and Te are both effectively lowered to the 1 to 5 ppm range in the overflow from the fourth aging tower. This ensures that copper cathodes can be plated within chemical quality specifications for Se and Te which are10 ppm and 5 ppm, respectively.

Electrowinning Process

Now that the pregnant electrolyte has been purified, the purpose of the Copper Electrowinning circuit is to properly prepare the solution and plate out the copper in the tankhouse. The purified pregnant electrolyte is first collected in a tank so that it is appropriately mixed with spent electrolyte and addition agents. Some addition agents include glue to improve profile smoothness of the cathodes during plating and an anti-misting solution called "Dowfax" to ameliorate work room conditions by suppressing acid mist generation. The prepared solution is then pumped through a set of plate and frame heat exchangers to a head tank. The heat exchangers effectively cool and control the temperature to around 55^{o}C. The head tank provides a constant head pressure in order to deliver regular feed flows to the electrowinning tankhouse.

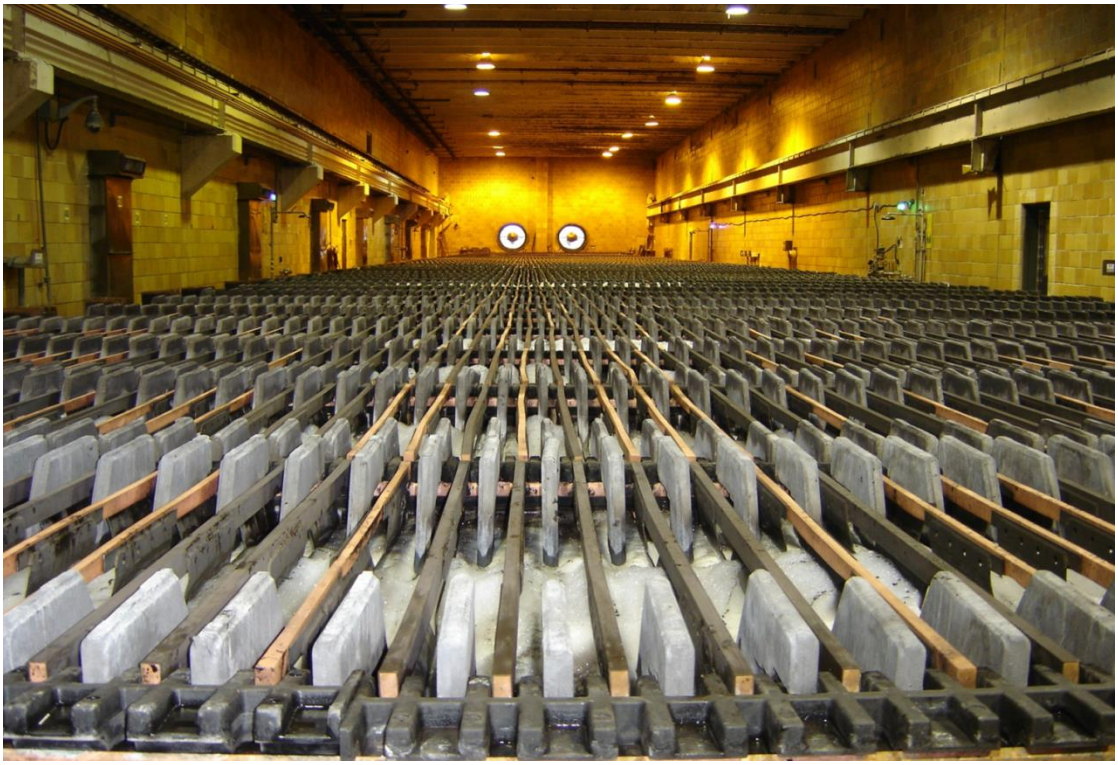

Figure 4: Photograph of Vale's electrowinning tankhouse

As shown in the figure above, Vale's copper electrowinning tankhouse contains 49 cells, each cell containing 66 titanium cathode blanks and 67 lead anodes. The DC current applied varies from 14,000 Amps if the operators are in the process of pulling finished cathodes to full power at night or weekends with 31,000 Amps. The electrolyte flow is easily maintained at 40 L/min by means of a weir positioned at the inlet of each cell.

As the pregnant (copper sulphate) electrolyte passes through the cell with the applied current, pure Cu metal is plated at the cathode by the following reaction:

$$2CuSO_4 + 2H_2O \rightarrow 2Cu + 2H_2SO_4 + O_2$$

Further to the reaction above, oxygen is also generated at the anode which often carries and creates the acid mist in the working environment. Other side reactions do occur in the tankhouse such as the reduction and/or oxidation of iron which can unfavorably affect the current efficiency. Therefore, in copper electrowinning it is also important to reduce Fe levels as well, to maximize the tankhouse potential to plate out copper. Cu is deposited on the cathode blanks for 17-20 days before it is pulled, washed, stripped and bundled for market as shown in figure below. Generally, the capacity of the tankhouse to plate copper is 60,000 to 65,000 lbs per day.

Figure 5: Cu cathodes for market

4.2 Variables

All data for this work was based from Vale's electrowinning process in Copper Cliff, Ontario. A year's worth of measurable data was collected from available instruments around the Se/Te Removal and Electrowinning Circuits. A sampling rate of 18 minutes was chosen as the tradeoff point for minimal noise and minimal loss of information.

For the same time period, data that was not continuously measured by instruments such as sample assays was also utilized in the experimental design. Depending on the location and criticality of the sample results, the sampling rate varies from every 6 hours to once a day. For example, the Copper Concentration in Tankhouse Feed is based on sample assays that are done by operators every 6 hours which are 20 times less frequent than other variables. Table 1 below lists the variables involved in the Se/Te removal and electrowinning process. The numerous variables and complex process are further simplified pictorially in Figure 6.

Table 1: List of variables for Se/Te removal and electrowinning process

Description	Unit	Symbol
Temperature of electrowinning tankhouse feed	^{o}C	T1
Temperture of spent electrolyte	^{o}C	T2
Feeding temperature to the Se/Te removal circuit	^{o}C	T_f
Feeding flow rate to the Se/Te removal circuit	L/min	F_f
Flow rate from underflow of #1 aging tower	L/min	F_{uf}
Glue addition rate	L/min	F_{glue}
Level in the Se/Te removal pump tank	%	L_{pump}
Level in electrowinning mix tank	%	L_{ew}
Level in the return electrolyte tank	%	L_{spent}
ORP measurement from #4 aging tower overflow	mV	ORP_{at}
Power rectifier voltage	Volts	V
Power rectifier current	Amps	I
Copper Concentration in tankhouse feed	g/L	$X1_{Cu}$
Selenium concentration in tankhouse feed	ppm	$X1_{Se}$
Tellurium concentration in tankhouse feed	ppm	$X1_{Te}$
Copper Concentration in spent electrolyte	g/L	$X2_{Cu}$
Selenium concentration in spent electrolyte	ppm	$X2_{Se}$
Tellurium concentration in spent electrolyte	ppm	$X2_{Te}$

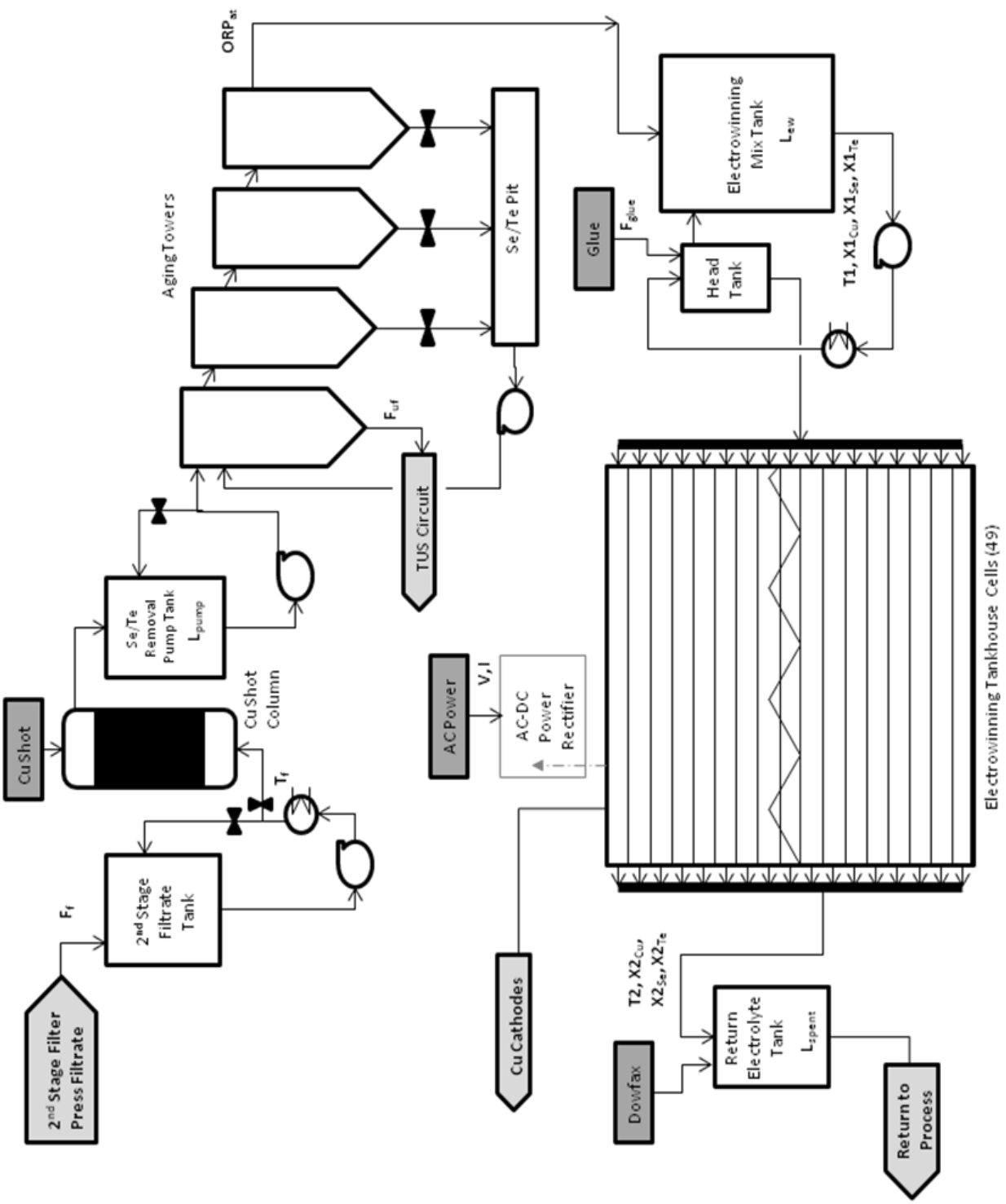

Figure 6: Se/Te removal and electrowinning process with indicated variable

Temperature of Electrowinning Tankhouse Feed (T_1)

The mixed electrolyte from the Electrowinning Mix Tank is pumped through heat exchangers to maintain temperature at approximately 60^{o}C. Note that spent electrolyte picks up heat as a consequence of the current applied in the tankhouse. When it is recycled back to the Electrowinning Mix Tank, the heat exchangers help to properly control the temperature and avoid an accumulation of heat before entering the tankhouse. Hence, this temperature measurement is a controlled variable. (Vale Ltd., 2012)

Temperature of Spent Electrolyte (T_2)

This temperature indicator designates the temperature of the spent electrolyte in the Return Electrolyte tank (measured variable). Due to the current supplied in the tankhouse, the temperature of the spent will be roughly 10^{o}C hotter than the tankhouse feed temperature. The temperature of the spent will run between 65 to 70^{o}C in normal conditions.

Feeding Temperature to the Se/Te Removal Circuit (T_f)

The temperature to the Se/Te Removal Circuit must be controlled to approximately 100^{o}C (controlled variable). If the feed temperature begins to drop below 95^{o}C, the rate of reaction decreases and the rate at which Se/Te precipitate out of solution decreases as well.

Feeding Flow Rate to the Se/Te Removal Circuit (F_f)

The rate of flow to the Se/Te Circuit is strongly dependent on the copper content in the return electrolyte (spent). The control room operator will adjust the flow rate to control the residence time of the electrolyte in the cell and in turn, how much copper may be depleted from solution (manipulated variable). Typically, 40-50 g/L copper is the target concentration range in the return electrolyte. In other words, if the copper concentration is well above 50 g/L, the operator will lower the feed flow rate to allow more residence time in the cells.

Flow Rate from Underflow of #1 Aging Tower (F_{uf})

The purpose of the aging towers is to allow time for the Se/Te solids (also known as Tower Underflow Solids - TUS) to precipitate and settle to the bottom of the cones. Approximately, once a shift, the solids from #2, #3 and #4 aging towers are drained to the Se/Te Pit and pumped back to #1 aging tower. When the #1 aging tower cone becomes full, the solids are then under flowed to the TUS Circuit for further processing (measured variable). Typically, #1 aging tower is under flowed to the TUS Circuit 3 to 5 times per week.

Glue Addition Rate (F_{glue})

Animal glue is added to Head Tank as a surface leveling agent to provide aesthetically smooth finished copper cathode. If not enough or too much glue is added, it can result in nodule formation on the cathodes (controlled variable). Nodulated copper cathodes are unfavourable with customers and severely nodulated cathodes would be effectively reverted as scrap.

Level in the Se/Te Removal Pump Tank (L_{pump})

The Se/Te Removal Pump Tank acts a surge tank between the Cu Shot Column and the Aging towers. The level is maintained and flow to aging towers is controlled by manipulating Se/Te Removal pumps and an automatic valve on recycle line (controlled variable).

Level in the Electrowinning Mix Tank (L_{ew})

The Electrowinning Mix Tank is a storage tank for the purified pregnant copper electrolyte from the Se/Te Circuit. Often spent electrolyte from the Return Electrolyte tank is also recycled back to this tank so that it can have another pass through the tankhouse (controlled variable).

Level in the Return Electrolyte Tank (L_{spent})

The Return Electrolyte Tank acts as a surge tank before the spent is recycled to other locations. The majority of the spent is recycled to the electrowinning mix tank but it can be directed to the second stage mix tank, second stage filter press feed tank or the first stage mix tank as a bleed stream. As the level in the tank runs high, an automatic valve on the recycle line to the electrowinning mix tank will open to control and maintain the level. Typically, the level in the return electrolyte tank is controlled at 60% capacity (controlled variable).

ORP measurement from #4 Aging Tower Overflow (ORP_{at})

The online ORP (Oxidation-Reduction Potential) measurement at the overflow of #4 aging tower is an implied performance indicator. In this case, the ORP meter indicates the rate of reduction of Se and Te. If the ORP is less than 200 mV, then most of the Se and Te has been reduced and precipitated to a solid form. On the other hand, a high ORP signifies that Se and Te are remaining in solution, leaving the potential for Se and Te to be deposited on the cathodes in the tankhouse (measured variable).

Power Rectifier Voltage (V)

In order for copper electrowinning to take place, a voltage of ~ 2V per cell must be applied to overcome losses due to electrolyte resistance, kinetic and mass transfer limitations. Generally, the rectifier produces 13,800V AC power down to 150V AC power and subsequently converts this AC power to DC power for electrowinning application (measured variable).

Power Rectifier Current (I)

The rectifier also regulates the DC power to provide a constant DC current. This current is then supplied to the tankhouse cells by means of positive and negative bus bars. Typical operation is 14,000 amps when operators are in the tankhouse stripping copper and up to

31,000 amps at full power (nights and weekends). A higher current will allow more copper to plate out of solution but other factors can impact current efficiency. For example, iron in electrolyte has a negative effect on current efficiency because as the ferrous ions become reduced, it consumes current that could have otherwise plated out more copper (controlled variable).

Copper Concentration in Tankhouse Feed ($X1_{Cu}$)

Every 6 hours samples are taken of the tank house feed by the chemical operators and analyzed for both copper and acid content. An indicator of good operation is that the copper content falls within desired range. Generally, the copper content and acid content falls in the range of 50-65 g/L and 180-220 g/L, respectively (measured variable).

Selenium & Tellurium Concentration in Tankhouse Feed ($X1_{Se}$, $X1_{Te}$)

Once a day, a grab sample is taken from the #4 aging tower overflows by chemical operators and sent for selenium and tellurium analysis. This analysis helps to monitor the performance of the Se/Te removal circuit to effectively remove/precipitate Se and Te out of solution. If Se and Te are relatively high in solution (> 5ppm) this could be subsequently plated in the tankhouse and accumulate to a point of causing chemically off-spec copper cathodes (measured variable).

Copper Concentration in Spent Electrolyte ($X2_{Cu}$)

Regular samples are taken by the operator of the return spent electrolyte and analyzed for both copper ($X2_{Cu2}$) and acid content. The spent is also analyzed for copper ($X2_{Cu}$) on a more continuous basis using an online Cu analyzer to compare with the operator assays. Measuring the copper concentration in the spent is a critical performance indicator to operations. The Cu concentration determines how much Cu is being plated and whether adjustments need to be made (controlled variable). For example, the feed flow rate to the Se/Te removal circuit may need to be adjusted to alter the residence time or current may need to be reworked to change the amount being plated. Note plating down to 10 g/L Cu in the spent can introduce other dangers such as the formation of toxic arsine gas (formed when arsenic comes into contact with acid at high power and low Cu concentration).

Selenium & Tellurium Concentration in Spent Electrolyte ($X2_{Se}$, $X2_{Te}$)

Four times a day, a sample is taken from the return electrolyte tank. A cut of each sample is combined together to form a daily composite sample that is submitted to the lab for analysis. The Se and Te assays help to monitor how much remains in solution after electrodeposition. This becomes especially important during an upset condition to help predict how much the Se and/or Te will affect the quality of the copper cathodes (measured variable).

Chapter 5: **Dynamic Modeling**

At Vale Canada's Copper Electrowinning plant, the sulphide residue feed - containing Cu, Ni, Co, Fe, precious metals and other impurities - is subjected to a series of leaching steps to effectively separate and concentrate the metals. The final leach before electrowinning is an oxidative pressure leach to produce a relatively pure copper sulphate solution. Remaining impurities in the solution that require removal are mainly selenium (Se) and tellurium (Te). Under very strict conditions, Se and Te can be efficiently precipitated out of solution by means of cementation and settling. It is very important to reduce Se and Te to low concentrations in solution; otherwise they will contaminate the copper cathodes. After passing through the Se/Te removal circuit, the pregnant electrolyte contains less than 5 ppm Se/Te. The electrolyte then enters the electrowinning operation for copper plating. The electrowinning operation is the final step in generating high purity Cu product and it is, therefore, essential to make continued efforts in understanding the process and improving the operation. Modeling of the process helps to enhance our understanding of the process and provide insight to possible process improvement and process control development.

Efforts have been made in modeling electrowinning operations by various research and industrial groups (Aminian, et al., 2000). Process modeling is generally categorized into

steady state or dynamic modeling. Although steady state models are commonly simpler and easier to set up, they are more applicable for design work where the process does not fluctuate dramatically. Most existing models for copper electrowinning processes have been focused on steady state operations where variable variations with time are not considered. Hydrometallurgical processes include much complexity as a result of handling multiple-state feeds (i.e. solid-liquid slurry), multiple phase reactions and corrosive environments that occur throughout each circuit. Furthermore, the variability in the feed parameters or ore types can also change process conditions on a day-to-day basis, making it even more difficult to use standardized flow sheets or equipment. For these reasons, the need for dynamic modeling of hydrometallurgical processes is well known but limited in comparison to other chemical industries. It is, therefore, of great interest to investigate dynamic modeling of the copper electrowinning with validation of industrial time series data.

In this chapter, dynamic modeling of copper electrowinning operations is carried out using mass and energy conservation and Faraday's Law. The focus of modeling is to capture essential dynamics of copper concentration and temperature for process monitoring and control purposes. The combined first principle and data based model obtained takes the form of partial differential equations (PDEs) describing how copper concentration and temperature vary with time under various operating conditions. The resulting model can be used to predict dynamic variation of output such as electrolyte concentration and cell temperature under given electrowinning inlet conditions. It can also be used to provide a more continuous estimate for variables that are measured infrequently. For example, at the Vale

Electrowinning Plant, the current tankhouse feed copper concentration is only measured four times a day. The proposed models not only quantify the effects of the process inputs on the process outputs, but also help to monitor those variables that are not measured on a continuous basis (online). In this chapter, dynamic models for copper concentration in tankhouse feed and temperature of electrolyte are developed and the models are validated with industrial operating data. The models are also used to estimate the feed concentration that is not measured online. Simulations of the models are performed to investigate the variable profile dynamics under various operating conditions.

5.1 Dynamic Model Development

The main reduction and oxidation reactions that take place at the cathode and anode, respectively, include (Aminian, et al., 2000):

Reduction of cupric to elemental copper: $Cu^{2+} + 2e^{-} \rightarrow Cu$

Oxidation of water to hydrogen ions: $H_2O \rightarrow \frac{1}{2}O_2 + 2H^{+} + 2e^{-}$

Most copper electrowinning process models are initiated from mass and energy conservation laws as well as Faraday's Law.

5.1.1 Model for copper concentration

A model for copper concentration is developed by applying the mass conservation on an electrolytic solution in the cell. In the electrowinning cell, the solution enters the cell with higher copper concentration. The copper concentration decreases along the direction of

solution flow in the cell. In order to describe the concentration variation along the flow direction, the electrolyte is divided into a large number of thin layers in the flow direction. Considering one layer of electrolyte (as in Figure 7) where the coordinate direction z is set the same as flow direction:

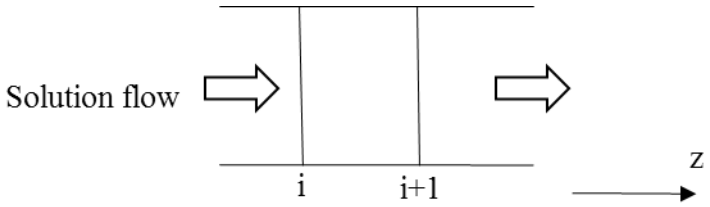

Figure 7: Flow through a thin layer of electrolyte

Applying mass conservation for copper component in the thin layer of the electrolyte, it is obtained:

$$\frac{(\Delta zA)(X_{Cu,t+1} - X_{Cu,t})}{\Delta t} = uA(X_{Cu,i} - X_{Cu,i+1}) - \frac{P}{V}(\Delta zA) \qquad (5.1)$$

where V indicates volume of the electrolyte (m^3), A is the cross-sectional area of the cell (m^2), u is the flow speed (m/s), X_{Cu} indicates the copper concentration (g/m^3), Δz is the distance between node i to node $i+1$ (m), Δt is the time difference (s), P is the rate of copper deposition (g/s). The rate of copper deposition is realized by Faraday's Law:

$$P = \frac{M_{Cu}\phi I}{ZF} \qquad (5.2)$$

where M_{Cu} is the molecular weight of Cu (g/mol), I is the total electric current applied to the cell (A), F is the Faraday's constant 96,500 (C/mol), Z is the number of electrons involved in

the copper deposition reaction and ϕ is the current efficiency of copper to deposit on cathodes.

Reorganizing Equation (5.1) and let $\Delta t \to 0$ and $\Delta z \to 0$, a partial differential equation model for copper concentration is then obtained:

$$\frac{\partial X_{Cu}}{\partial t} + u\frac{\partial X_{Cu}}{\partial z} = -\frac{M_{Cu}\phi I}{ZVF} \tag{5.3}$$

The boundary condition for the above equation can be written as:

$$\begin{cases} X(z=0) = X1_{Cu} \\ X(z=L) = X2_{Cu} \end{cases} \tag{5.4}$$

where $X1_{Cu}$ is the copper inlet concentration and $X2_{Cu}$ is the copper outlet concentration. The model represented in (5.3) and (5.4) describes how copper concentration varies with time as well as along the flow direction.

For the copper electrowinning application, it is desirable to obtain the relation of copper outlet concentration $X2_{Cu}$ with inlet concentration $X1_{Cu}$ and current I. This can be achieved by solving Equation (5.3) using the method of characteristics, which converts (5.3) into a group of ordinary equations:

$$\begin{cases} \dot{t} = 1 \\ \dot{z} = u \\ \dot{X}_{Cu} = -\dfrac{M_{Cu}\phi I}{ZVF} \end{cases} \tag{5.5}$$

In the development of this model, several assumptions were made. For instance, the variation of the current was assumed to be constant within one residence time. Also, copper diffusion

was considered negligible. Integrating the above equation for the length of residence time yields:

$$X2_{Cu}(t+t_R) = X1_{Cu}(t) - \frac{M_{Cu}\phi t_R}{ZVF} I(t) \tag{5.6}$$

where t_R denotes the residence time. Equation (5.6) describes how copper outlet concentration relates with the inlet concentration, current and other parameters.

In the above model development, eddy diffusion was not included. Including diffusion into the model, Equation (5.3) becomes:

$$\frac{\partial X_{Cu}}{\partial t} + u\frac{\partial X_{Cu}}{\partial z} - D\frac{\partial^2 X_{Cu}}{\partial z^2} = -\frac{M_{Cu}\phi I}{ZVF} \tag{5.7}$$

where D (m^2/min) denotes the eddy diffusivity coefficient brought on by the turbulence of the rising bubbles . In Equation (5.7), the term $u\frac{\partial X_{Cu}}{\partial z}$ represents the concentration variation due to convection, the term $D\frac{\partial^2 X_{Cu}}{\partial z^2}$ represents the concentration variation due to eddy diffusion, and the term $-\frac{M_{Cu}\phi I}{ZVF}$ represents the copper concentration decrease due to electrowinning reaction. The applied rectifier power current is closely related to how much Cu from the tankhouse feed deposits via Faraday's Law. Copper diffusion in the solution is inevitable; Equation (5.7) is thus a more accurate model than Equation (5.3). It is, however, not straightforward to solve the parabolic partial differential equation (5.7) analytically. With known parameters, it can be solved using numerical approaches and be used to investigate

the copper concentration variation under various conditions. In some real applications, the effect of convection is much more dominant over that of diffusion; the model of copper concentration can be represented using Equation (5.3).

For the developed model, it is critical to estimate the model parameters that reflect the industrial operation. Using the model in (5.6), the model parameters can be conveniently estimated with industrial measurements. In the copper electrowinning plant, copper inlet and outlet concentrations are usually measured. Assuming that the volume V, residence time t_R and ϕ are relatively kept constant, let:

$$\alpha = -\frac{M_{Cu}\phi t_R}{ZVF}$$

Equation (5.6) becomes:

$$X2_{Cu}(t+t_R) = X1_{Cu}(t) + \alpha I(t) \qquad (5.8)$$

It is noted that the assumption of current efficiency ϕ being constant may not be accurate. In this chapter, variation of current efficiency ϕ is not considered. Based on measured data of $X2_{Cu}$, $X1_{Cu}$ and current I, the parameter α can be estimated using the least square approach if the residence time t_R is known. Estimation of the residence time t_R can be obtained by different approaches. If the volume V of electrolyte and flow rate Q is known with reasonable accuracy, the residence time can be estimated by $t_R = \frac{V}{Q}$. The volume V of electrolyte is the tank volume minus the volume of electrodes. With volume variation of electrodes, the volume V of electrolyte is unknown, but a reasonable initial estimate for the residence time t_R can be obtained by approximating the volume V of electrolyte by the tank volume. The

residence time t_R can also be estimated by solving t_R such that the correlation between $X2_{Cu}(t+t_R) - X1_{Cu}(t)$ and current *I(t)* be maximum for the industrial operating data, i.e.,

$$\max_{t_R} \frac{\sum_t \left[\left(X2_{Cu}(t+t_R) - X1_{Cu}(t)\right) - \left(\bar{X}2_{Cu} - \bar{X}1_{Cu}\right)\right]\left[I(t) - \bar{I}\right]}{\sum_t \sqrt{\left[\left(X2_{Cu}(t+t_R) - X1_{Cu}(t)\right) - \left(\bar{X}2_{Cu} - \bar{X}1_{Cu}\right)\right]^2 \sqrt{\left[I(t) - \bar{I}\right]^2}}} \qquad (5.9)$$

A simpler version of the second approach is to use the trial and error such that the model predicted data fits well with the industrial operating data for Equation (5.8). The second approach was used in the model to estimate t_R parameter as it did provide a better fit to the industrial operating data in comparison to the first approach and less cumbersome calculation. In this case, the residence time across a cell is assumed constant and the change of volume due to cathode growth is negligible. With the estimated parameters α and t_R, copper leaving the tankhouse can be predicted from Equation (5.8) based on the tankhouse feed and applied current. In the Copper Cliff Electrowinning plant, the copper outlet concentration $X2_{Cu}$ and current I are measured online continuously, but the feed concentration of copper is only measured 4 times a day. Based on the estimated parameters and Equation (5.8), the missing measurement for feed concentration $X1_{Cu}$ can be estimated from the online measurement of outlet concentration $X2_{Cu}$ and current I.

5.1.2 Model for temperature

In the electrowinning process, temperature is an important variable to be monitored. The temperature increment in the electrowinning tank mainly results from current. In modeling the temperature variation in this chapter, the contribution from the current is included and

other contributions are assumed negligible. For simplicity of model development, the temperature is first modeled without including the effect of thermal diffusion. Similar to modeling of the copper concentration in the last subsection, temperature is modeled by applying energy conservation around the thin layer of the electrolyte as illustrated in Figure 7

$$\frac{(\Delta zA)(\rho c_p T_{t+1} - \rho c_p T_t)}{\Delta t} = \rho c_p uA(T_i - T_{i+1}) + \frac{I^2 R}{V}(\Delta zA) \tag{5.10}$$

where T indicates temperature (^{o}C), ρ is density of the electrolyte (kg/m^3), c_p is the specific heat coefficient, R is the resistance (Ω). It is assumed that density ρ and the specific heat coefficient c_p are constant. Let $\Delta t \to 0$ and $\Delta z \to 0$, a hyperbolic partial different equation model for the temperature is obtained:

$$\frac{\partial T}{\partial t} + u\frac{\partial T}{\partial z} = \frac{I^2 R}{\rho c_p V} \tag{5.11}$$

with the boundary conditions:

$$\begin{cases} T(z=0,t) = T_1(t) \\ T(z=L,t) = T_2(t) \end{cases} \tag{5.12}$$

where T_1 denotes the inlet temperature and T_2 is the outlet temperature. Using the method of characteristics, the outlet temperature T_2 can be expressed as:

$$T_2(t + t_R) = T_1(t) + \frac{Rt_R}{\rho c_p V} I^2(t) \tag{5.13}$$

Assuming the volume V, residence time t_R and resistance R is relatively constant, define a parameter:

$$\beta = \frac{Rt_R}{\rho c_p V}$$

Equation (5.6) becomes:

$$T_2(t + t_R) = T_1(t) + \beta I^2(t) \tag{5.14}$$

In the above model development for temperature, the effect of thermal diffusivity is not included. The effect of thermal diffusivity can be included in the model by adding the diffusion term in Equation (5.11), leading to:

$$\frac{\partial T}{\partial t} + u\frac{\partial T}{\partial z} - D_T\frac{\partial^2 T}{\partial z^2} = \frac{I^2 R}{\rho c_p V} \tag{5.15}$$

where D_T denotes the eddy thermal diffusivity coefficient brought on by the turbulence in the cell. If the model parameters and boundary conditions are known, Equation (5.15) can be used to determine the temperature profile in the electrolyte cell. When the effect of convection is much more dominant than that of eddy diffusivity, Equation (5.15) can be approximately replaced by (5.11).

5.2 Model Validation

For parameters estimation and model validation, one year's worth of industrial operating data was utilized. A sampling time of 18 min was used in data collection for continuous measurements such as current *I*, temperature *T*, and copper concentration of spent electrolyte ($X2_{Cu}$). For copper concentration, Equation (5.8) is used to estimate the parameters and model validation. As current *I* and copper concentration of spent electrolyte ($X2_{Cu}$) are measured continuously but the feed concentration is only measured infrequently. As a result, *I* and $X2_{Cu}$ were reduced to match the same frequency as copper concentration of tankhouse feed for parameter identification. The residence time t_R was estimated using "trial and error".

The least square approach was then used to estimate the parameter α. With the parameters estimated, Equation (5.8) can be used to predict copper concentration out of the tank from the feed condition and the applied current. Equation (5.8) also provides a way to estimate the feed concentration that is not measured online from the online measurement of I and $X2_{Cu}$:

$$\hat{X}1_{Cu}(t) = X2_{Cu}(t + t_R) - \alpha I(t) \qquad (5.16)$$

where $\hat{X}1_{Cu}$ indicates the model estimate value of feed concentration. By applying the above equation, the concentration of Cu in the tankhouse feed supplying the tankhouse can be determined using both current applied to tankhouse and spent electrolyte Cu concentrations. Online estimation of feed concentration data can then be obtained.

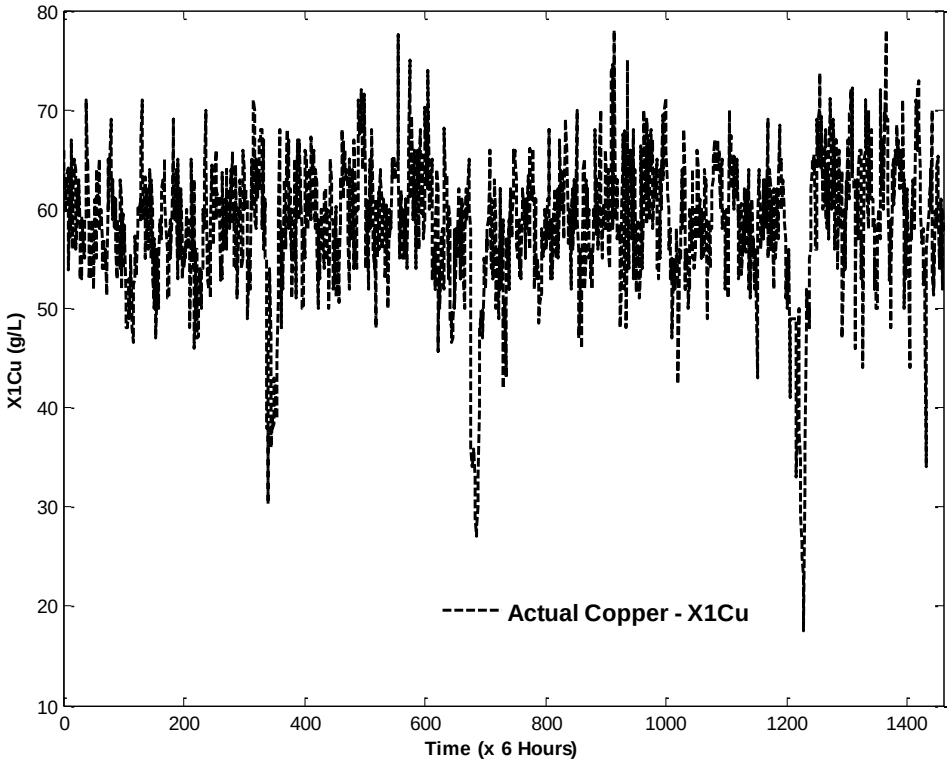

Figure 8: Copper concentration of tankhouse feed ($X1_{Cu}$)

To examine whether the model prediction was reliable with any data, the data collected for this work was split in half. The first half of collected data was used to estimate parameters while the second half was applied to validate whether the model predicted data fit with the industrial measured data. Figure 8 and Figure 9 displays the actual copper concentration (dashed line) of the tankhouse feed collected from the process and the model estimated concentration (solid line). Figure 8 shows the concentration for the full year, where the parameter α is estimated from the measurement data of the first half year, while Figure 9

displays the predicted concentration from the estimated parameter α obtained from the first half year's data in comparison with actual concentration.

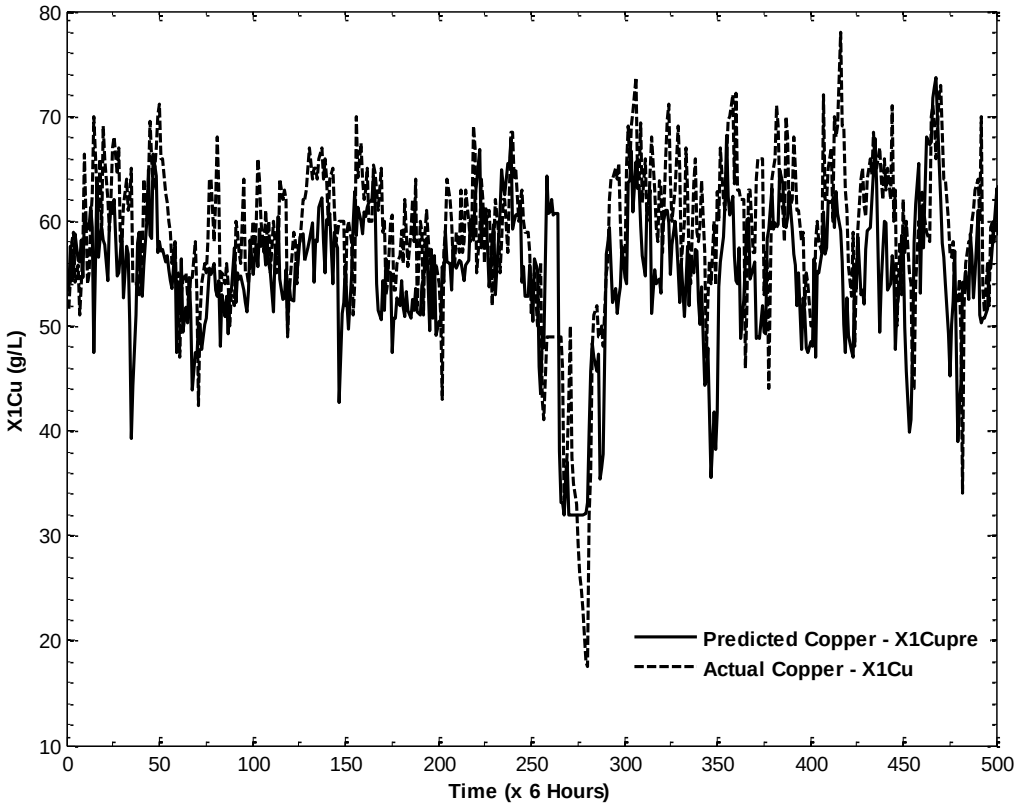

Figure 9: Model prediction of tankhouse feed copper concentration ($X1_{Cu}$ and $X1_{Cupre}$)

Clearly both Figure 8 and Figure 9 demonstrate that the model was able to closely imitate the actual Cu concentrations in the tankhouse feed. For Figure 9, the correlation between actual $X1_{Cu}$ and predicted $\hat{X}1_{Cu}$ was calculated as 0.74 which is an impressive fit, considering the variable peaks and drops in copper concentration of the process. The model effectively predicts fluctuations in concentration but for the most part at a lower magnitude. A biased low number could be more desirable as it provides a worst case scenario. However, the bias

is particularly consistent so it may be favorable to take the bias into consideration for future model development.

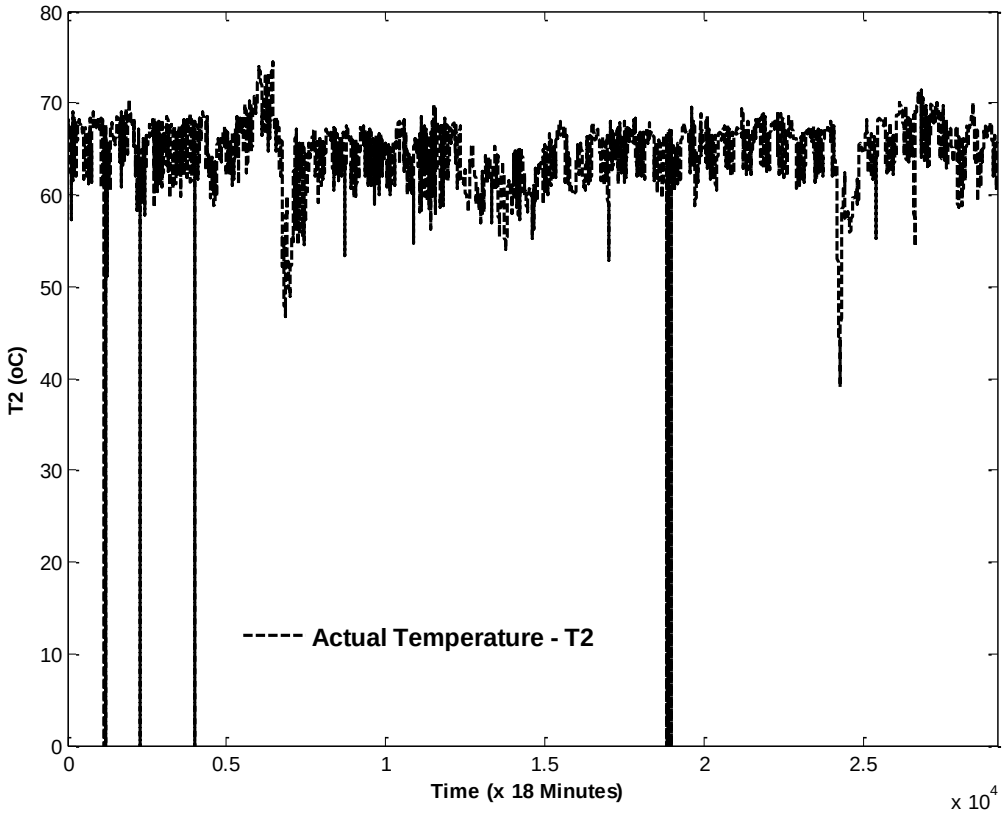

Figure 10: Temperature of spent electrolyte (T_2)

In order to ensure optimum deposit morphology, it is important to have good management of electrolyte temperature. A high temperature can increase surface diffusion of ad-atoms which in turn leads to nodulated growth on the cathodes. As such, a model (as discussed in previous section) was developed to predict the temperature of the spent electrolyte based on current I and temperature of tankhouse feed T_1. Figure 10 represents the actual full temperature data

set collected from the process, where the parameter β was estimated using the first half year's measurement data. Figure 11 demonstrates a comparison between predicted temperature utilizing this model ($\hat{T}_2$ or T_{2pre}) and the actual industrial data collected (T_2) for the second half year.

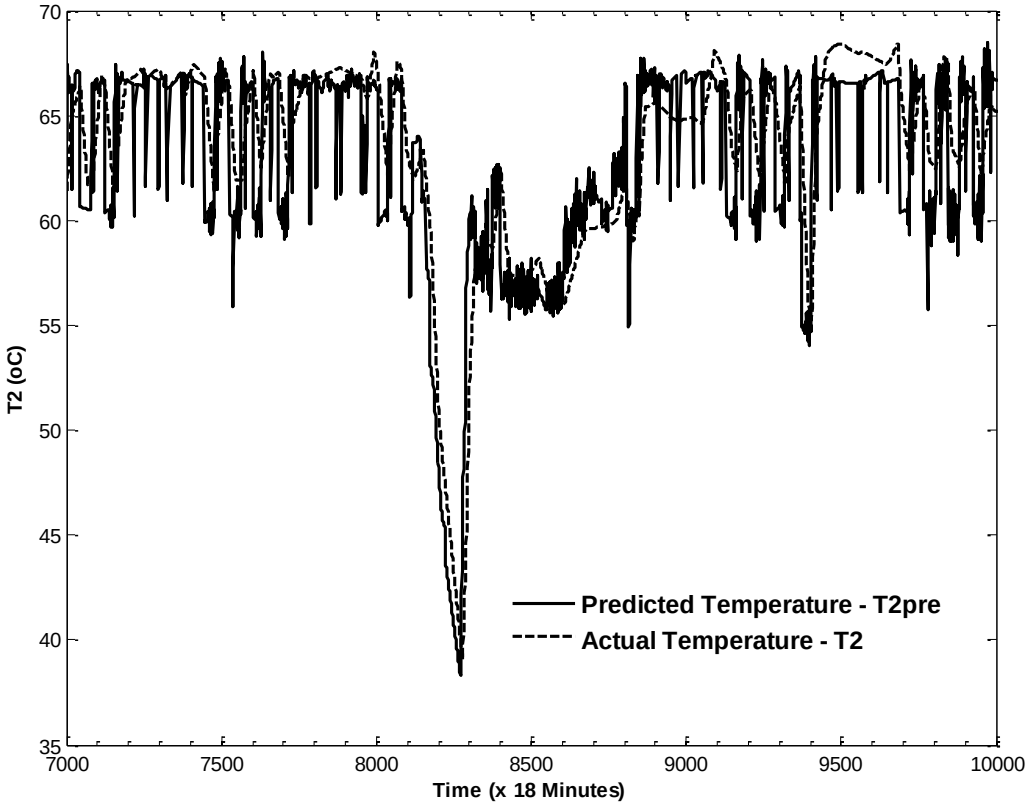

Figure 11: Model prediction of spent electrolyte temperature (T_2)

This figure noticeably demonstrates a close correlation of the model to the data set. The correlation between actual T_1 and predicted $\hat{T}_2$ for this 3000 data point time range was calculated as 0.73. Unlike the copper concentration model, there does not appear to be a bias

in estimating a lower or higher temperature than actuality. Furthermore, the model is consistently reliable in predicting any sustained drops in temperature that lasts longer than a few hours. There are however several drops in temperature for short periods of time that are predicted but do not appear in the actual data set. These almost instant drops in temperature are a most likely a result of power downs to perform physical cell flow checks. This does not necessarily hinder the model's usefulness but may require future modifications to decrease the noise.

5.3 Simulation

In section 5.1, dynamic models for copper concentration and temperature were developed in the form of hyperbolic PDEs and parabolic PDEs. If the effect of diffusion is negligible, the hyperbolic PDE models can be used to describe the variable variations in the copper electrowinning process. If the effect of diffusion is significant, the parabolic PDE model including a term of diffusion must be applied. An analytical solution was generated for the hyperbolic PDE models, and based on the solution, the model was validated by industrial operating measurement data in the previous section. In this section, simulations are run to investigate the copper concentration and temperature profiles in the electrowinning tank house. Effects of diffusion as well as that of other parameters are also explored based on simulations.

For the purpose of simulation, the values of model parameters were selected but may not necessarily reflect the operation in Vale’s Copper Cliff electrowinning plant. In this chapter,

the parameters were set as *u=0.025 m/min*, the length of the tank *L=7.5 m*. For simulation of copper concentration, feed concentration $X1_{Cu}$=60 g/L were used. It was found that literature values of diffusivity D for copper solution vary largely (Quickenden & Jiang, 1984; Hinatsul & Foulkes, 1989). For the simulation in this chapter, a larger value $D = 8\times10^{-10}\,\mathrm{m}^2/\mathrm{s} = 4.8\times10^{-8}\,\mathrm{m}^2/\mathrm{min}$, reflecting a worst scenario, was used. The parameters in the term $\frac{M_{Cu}\phi I}{ZVF}$ in (5.3) and (5.6) for copper concentration are lumped and replaced by the estimated parameter α obtained from last section. Based on these parameters, the hyperbolic model (5.3) and the parabolic PDE model (5.7) for copper concentration were simulated using the finite difference method. Figure 12 shows the copper concentration profile when the applied current increases from 19,000 Amps to 31,000 Amps at t=0 min. It was found that there was no noticeable difference between the simulated profile using the model (5.3) and that using (5.7). This further confirms that the effect of diffusion on the concentration variation is negligible. From Figure 12, the far end of copper concentration decreases and converges to a steady state as the current decreases. At any fixed time, the concentration decreases linearly along the tank length.

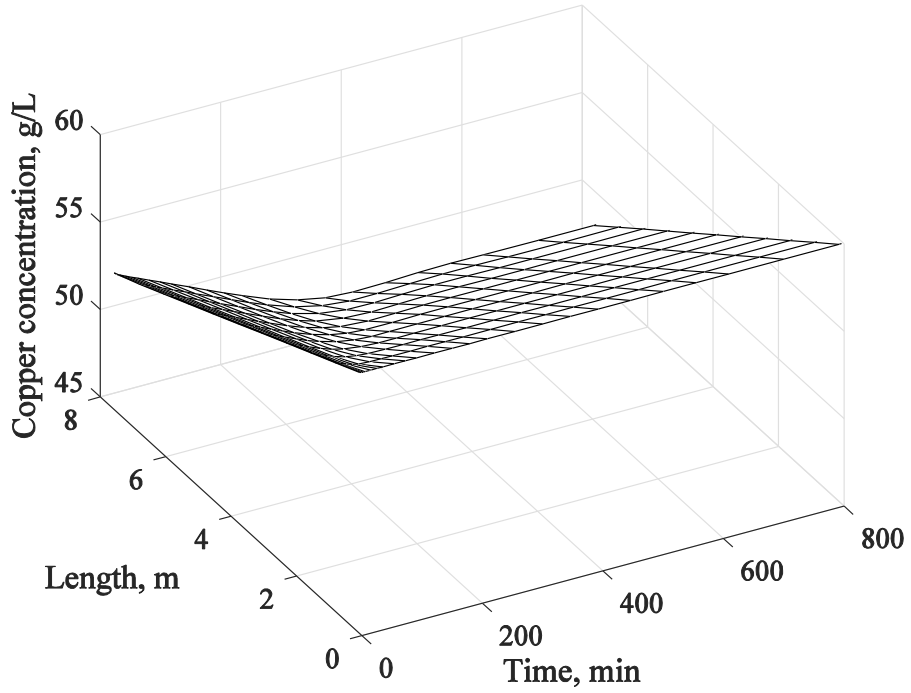

Figure 12: Copper concentration profile (u= 0.025 m/min, I = 19,000 Amps to 31, 000 Amps)

Effect of flow rate on the concentration profile was examined by setting the current to 31,000 Amps and letting flow speed decrease from 0.025m/min to 0.02 m/min. Figure 13 indicates the concentration variation when the flow speed decreases from 0.025m/min to 0.02 m/min. It is observed that the concentration is sensitive to variation of the flow rate and it decreases at the outlet end as the flow rate decreases. It is thus crucial to maintain stable and proper flow rate in order to make sure the copper concentration above the minimum requirement in the solution.

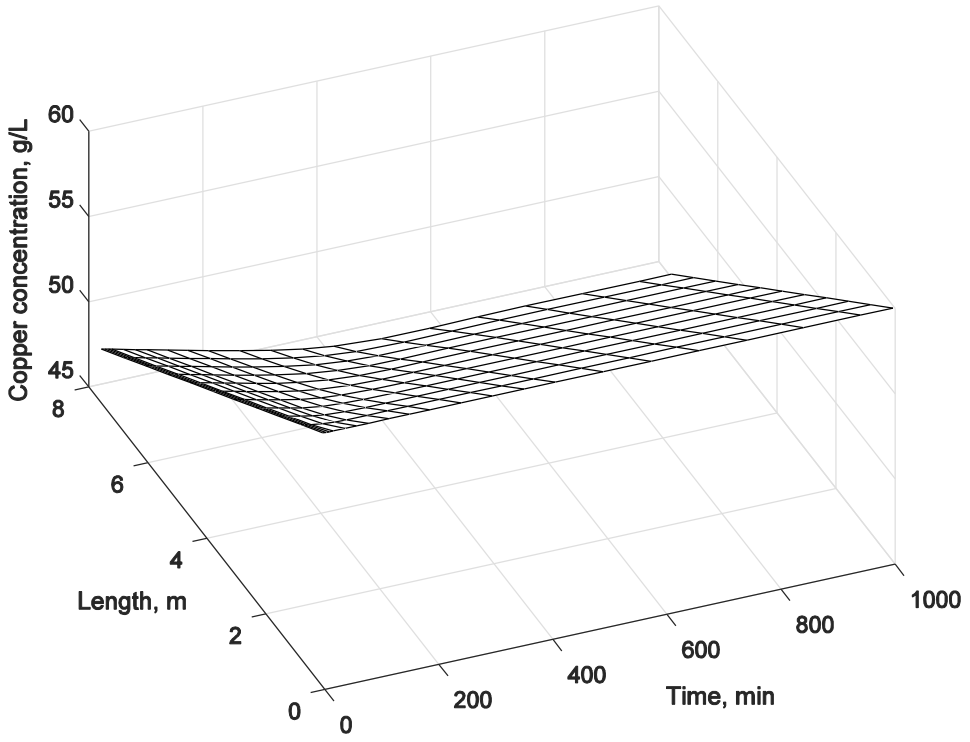

Figure 13: Copper concentration profile (I = 31, 000 Amps, u = 0.025 m/min to 0.020 m/min)

For simulation of temperature profile, the feed temperature T_1=55^{o}C was used. A larger parameter value $D_T = 1.6\times10^{-6}\,\mathrm{m}^2/\mathrm{s} = 9.6\times10^{-5}\,\mathrm{m}^2/\mathrm{min}$, representing a worst scenario for the thermal diffusivity of copper solution, was used to explore the effect of thermal diffusivity on the temperature variations. The parameters for the term $\frac{R}{\rho c_p V}$ in (5.13) and (5.15) is obtained from the estimated parameter β using the industrial operating data, as described in the last section. Figure 14 shows the temperature profile variation when the applied current increases from 19,000 Amps to 31,000 Amps at t=0 min. Comparison was

made on simulations based on the hyperbolic PDE model (5.13) without considering the effect of thermal diffusion or the parabolic PDE model (5.15) containing the effect of thermal diffusivity. No noticeable differences were observed in the temperature profile. As a matter of fact, even further increasing the value of D_T up to ten fold does not make difference in temperature variation in the tank. This implies that the effect of thermal diffusivity on the temperature in the electrowinning is negligible and the hyperbolic PDE model is adequate in representing the temperature variation in the electrowinning tank. From Figure 14, the temperature in the tank increases as the current increases from 19,000 Amps to 31,000 Amps. The further along the tank, the larger the increment.

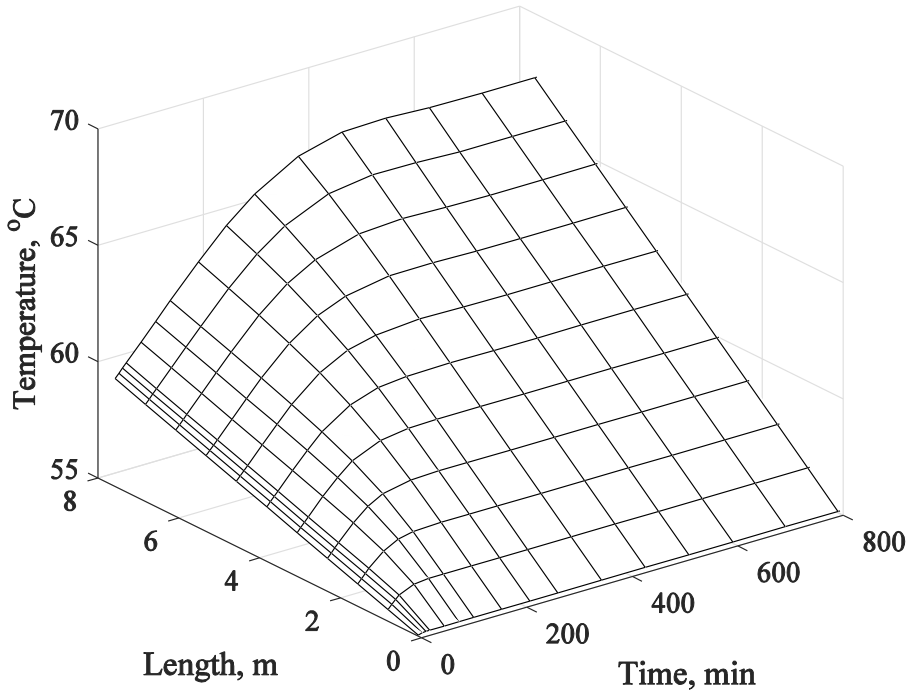

Figure 14: Temperature profile (u= 0.025 m/min, I = 19, 000 Amps to 31, 000 Amps)

Effect of flow rate on temperature is investigated by decreasing the flow rate from u = 0.025 m/min to u = 0.02 m/min while maintaining the current at 31,000 Amps, as shown in Figure 15. It can be seen that temperature increases greatly with the decrease of flow rate. Increment of temperature has the danger of increased mist in the air and thus maintaining a proper flow rate is crucial for the electrowinning operation.

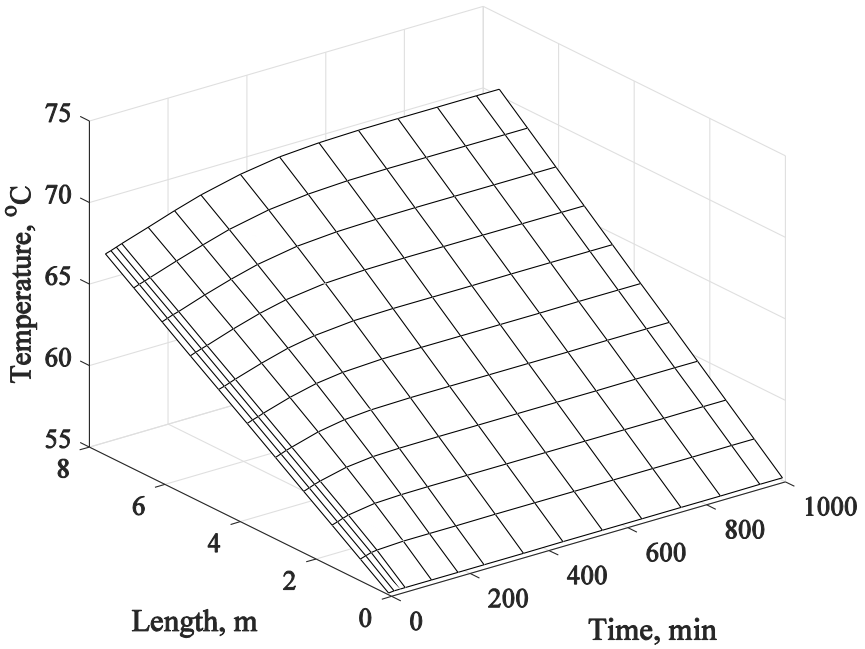

Figure 15: Temperature profile (I = 31,000 Amps, u = 0.025 m/min to 0.020 m/min)

5.4 Conclusions

In this chapter, dynamic models for copper concentration and temperature in the electrowinning tank are developed using mass and energy balance. When the effect of diffusion is not considered, the models take the form of first order hyperbolic PDEs. The

analytical solution for the hyperbolic model provides a convenient format for model validation with industrial operating data. Comparison with industrial measured data indicates that the developed model fits reasonably well with industrial operation. Simulation of the PDEs models shows that the effect of diffusion term in the parabolic model is negligible and the first order hyperbolic PDE models are adequate in describing variations of copper concentration and temperature. The developed models provide a useful tool in exploring variable profiles under various operating conditions.

In order to produce high quality cathodes, dynamic control and optimization of several parameters is required. Copper concentration in spent electrolyte is generally a more popular measurement to monitor as it provides an indication to operations if the electrolyte feed rate needs to be adjusted. However, copper concentration in the tankhouse feed is still a critical parameter as it completes the picture of the tankhouse for understanding performance upstream and downstream. For example, an increase in copper concentration can help explain improvements in current efficiency or reductions in energy consumption. On the flip side, copper concentration of the tankhouse feed determines the efficiency of the preceding circuit to leach out copper. Improving monitoring and control can evidently be very difficult when certain parameters are only available at discrete times. Unfortunately, sample preparation and analysis is cumbersome and can only be realistically provided at large time intervals. In conclusion, utilizing this model and estimating Cu concentrations at a higher frequency rate could be beneficial in improving monitoring and control of the tankhouse.

In copper electrowinning, temperature of the electrolyte can impact the mass transfer rates of copper ions and deposit morphology of the cathode surface. Electrolyte temperature range can vary plant to plant as there exists no optimum temperature range that applies to all since it can be affected by other operating parameters. In general, a lower temperature can cause a slower mass transfer rate but overall does not affect the plating rate of copper. Temperature may also play a part in electrolyte speciation specifically at the cathode surface. A higher temperature tends to decrease the electrolyte viscosity and the presence of ferric ion which will lead to a decrease of current efficiency. Although this model is not necessarily the most complex of electrowinning processes available, often a simpler model is easier for set-up and more likely sustained at the industrial site. The temperature model can then be a useful tool to understand fluctuations in the system and potential current efficiency opportunities.

Chapter 6: **Fault Detection and Diagnosis**

Copper electrowinning plants are where high purity Cu product is obtained through electrochemical reduction of copper from the leaching solution (Aminian, et al., 2000). Electrowinning recovers copper from solution obtained by leaching low grade copper ore or residues. Presence of selenium and tellurium in copper sulphide minerals results in contamination of pregnant leach solution. To ensure the copper product of desirable quality, selenium and tellurium have to be removed from the leach solution before the solution passes through electrowinning cells. The Se and Te removal and electrowinning process has a long residence time due to the slow and complicated reaction kinetics (Mokmeli, et al., 2014). Early detection and diagnosis of process faults is essential to avoid abnormal event progression and to produce copper products of consistent quality.

There is an abundance of literature on process fault detection and diagnosis ranging from analytical methods to artificial intelligence and statistical approaches. The analytical schemes for fault diagnosis are signal processing techniques using state estimation, parameter estimation, adaptive filtering and so on (Venkatasubramanian, et al., 2003). The key component in these schemes is diagnostic observers for residue generation. Some earlier work using diagnostic observers approach can be found in other articles (Clark, 1979; Frank, 1990; Massoumnia, 1986). Model-based diagnosis depends on the model reliability and model validity has been taken into account in fault detection and diagnosis (Lesecq & Gentil, 2008; Gentil, et al., 2009). Artificial neural networks (ANNs) have also been applied in fault

detection and diagnosis with the available online training methods (Ruiz, et al., 2000; Zhang, 2006). This approach requires a large amount of training samples, but signal samples with faults are usually very limited in the industrial applications. Other techniques such as Petri net and expert systems have been proposed to solve the problem for batch processes (Power & Bahri, 2004; Mehranbod, et al., 2005). Multivariate statistical process modeling methods have been extensively used in process monitoring and fault detection (Jackson, 1991; Lee, et al., 2004; Kourti & MacGregor, 1996). The methods are data-driven and one of the most commonly used tools is principal component analysis (PCA) (Wise & Gallagher, 1996; Russell, et al., 2000). In PCA based fault detection, PCA extracts the principal components of small dimension from data and a fault is detected by comparing a detection index with its control limit. Contributions of individual variables to the fault detection index are then calculated to diagnose the variables contributing to the fault (Alcala & Qin, 2011).

Dynamic principal component analysis (DPCA) is an extension of PCA to the realm of dynamic processes with serial correlation (Russell, et al., 2006). DPCA has been widely used in monitoring of dynamic multivariate processes and it was also used in disturbance detection and isolation (Ku, et al., 1995; Chen & Liu, 2002) . In comparison with the conventional PCA, DPCA uses time lagged information to acquire more reliable detection for dynamic systems. After a fault is detected, it is desirable to diagnose the root cause and identify faulty variables. As DPCA based methods construct detection indices using augmented variables, contribution analysis for diagnosis using DPCA is not a straightforward extension of that using the conventional PCA and limited results have been proposed (Li, et al., 2014). In the

existing research, algorithms of fault detection and diagnosis using DPCA have only been evaluated through simulations and applications to industrial systems have not been widely explored.

In this work, DPCA based fault detection and diagnosis is applied to an industrial Se/Te removal and Cu electrowinning process. Removal of Se/Te from the leaching solution requires long residence time due to its slow dynamics. By including a time lag window, DPCA is able to extract the reasonable data information for the process. The variables incorporating the time-lagged window are augmented with large dimension and DPCA is used to derive the principal components of reduced dimension. The Hotelling's T^2 statistic is then calculated for fault detection and the test results are validated with known industrial information. The fault is then further analyzed using contribution of individual variables to the Hotelling's T^2. In obtaining the contribution of each variable to the fault, a modified partial decomposition contribution is proposed to include all information within the time lag window. Application of fault detection and diagnosis to the industrial Se/Te removal and Cu electrowinning process may result in enhanced process operation and improved product quality with the faulty conditions being detected and removed in a timely manner.

6.1 DPCA based fault detection

A chemical process usually contains a large number of variables, and system diagnosis can thus be computationally demanding. PCA can be used to extract a small number of latent variables that explain most of the variance of the large data set and allow for a more compact

approximation of the data (Yoon & MacGregor, 2001). In the Se/Te removal and Cu electrowinning process, long residence time and slow dynamics are involved. It is, therefore, reasonable to analyze the process incorporating past time observations. Depending on the size of time-lagged window to be incorporated, this may result in significantly augmented data dimensions. DPCA is thus necessary to extract the data information with reduced dimension.

Mathematically, DPCA starts with forming a time-lagged window for each group of data in the reference database. For the reference data, several groups of process data at normal operations are collected from the industrial Se/Te removal and Cu electrowinning process. The variable vector is denoted as $\mathbf{x} \in R^m$. In applying DPCA, the variables are augmented to include the previous d observations, i.e.,

$$x_d(i) = \begin{bmatrix} x^T(i) & x^T(i-1) & \cdots & x^T(i-d) \end{bmatrix}^T \in R^{m(d+1)} \tag{6.1}$$

where i indicates the current time instant. The data matrix with the previous d observations can then be written as

$$X_d = \begin{bmatrix} x^T(d+1) & x^T(d) & \cdots & x^T(1) \\ x^T(d+2) & x^T(d+1) & \cdots & x^T(2) \\ \vdots & \vdots & & \vdots \\ x^T(N) & x^T(N-1) & & x^T(N-d) \end{bmatrix} \tag{6.2}$$

where N indicates the number of observations. The covariance matrix of the time lagged data X_d is

$$S = \frac{1}{N-d-1} X_d^T X_d \tag{6.3}$$

If I groups of data at normal operations are collected as reference data and S_j indicates the covariance matrix corresponding to the j^{th} group, the average value of S is obtained:

$$S^{avg} = \frac{(N-d-1)}{I(N-d)} \sum_{j=1}^{I} S_j \tag{6.4}$$

Eigenvalues and eigenvector of the covariance matrix S^{avg} may be calculated. Let p_j indicate the eigenvector corresponding to the j^{th} largest eigenvalue λ_j and the j^{th} principal component is described by

$$t_j(i) = p_j^T x_d(i)$$

If the eigenvector p_k is normalized to a unit length, the variance of t_k is λ_k , that is, var(t_k) = λ_k. By arranging the eigenvalues in the order from the largest to the smallest, the first few principal components account for most variations in the augmented variables $\mathbf{x}_d$. The variation represented by the k^{th} principal component can be calculated using the following relationship:

$$\%Variation_{t_k} = \frac{\lambda_k}{\sum_j \lambda_j} 100\% = \frac{\lambda_k}{trace(S_{avg})} 100\% \tag{6.5}$$

To reduce the computation cost, the number of principal components can be set small. If the first a principal components contain most data information, e.g.,

$$\sum_{k=1}^{a} \%Variation_{t_k} \succ 90\%$$

it is necessary to choose the a largest eigenvalues and eigenvectors.

Corresponding to *a* largest eigenvalues, the data matrix X_d can be approximately represented by *a* principal components. Let Λ be a diagonal matrix containing the *a* largest eigenvalues and $P = [p_1, p_2, ..., p_a]$ containing the loading vectors associated with the *a* largest eigenvalues. The normal operation can be characterized by the Hotelling's T^2 statistic

$$T^2(i) = x_d(i)^T P \Lambda^{-1} P^T x_d(i) \tag{6.6}$$

The threshold value T_α^2 is calculated using the probability distribution:

$$T_\alpha^2 = \frac{a(N-d-1)(N-d+1)}{(N-d)(N-d-a)} F_{a,N-d-a,\alpha} \tag{6.7}$$

where α is the confidence level which is generally set as 95% and $F_{a,K-d-a,\alpha}$ is the F-distribution above the critical point α with *a* and $N-d$ - *a* degrees of freedom. By calculating real-time Hotelling's T^2 statistic, fault detection can be performed

$$T^2(i) \begin{cases} \leq T_\alpha^2 & fault\ free \\ > T_\alpha^2 & fault \end{cases} \tag{6.8}$$

Based on the obtained principal components from DPCA, faults detection can also be carried out using the squared prediction error (SPE). SPE is the sum of squares of prediction error over all variables:

$$SPE = \mathbf{r}^T\mathbf{r} \quad \text{and} \quad \mathbf{r} = (I - PP^T)\mathbf{x}_d \tag{6.9}$$

where **r** is the residual vector. The threshold of SPE can be determined as(Villegas, et al., 2010):

$$SPE_\propto = \frac{a(N-d-1)(N-d+1)}{(N-d)(N-d-a)} \theta_1 \left(\frac{N_\alpha \theta_1 h(2\theta_2)^{0.5} + \theta_1^2 + \theta_2 h(h-1)}{\theta_1^2}\right)^{1/h} \tag{6.10}$$

where N_α is the normal distribution with confidence limit α, and the parameters in equation above are calculated as:

$$\theta_1 = \sum_{j=a+1}^{m\,x\,(d+1)} \lambda_j$$

$$\theta_2 = \sum_{j=a+1}^{m\,x\,(d+1)} {\lambda_j}^2$$

$$\theta_3 = \sum_{j=a+1}^{m\,x\,(d+1)} {\lambda_j}^3 \qquad (6.11)$$

$$h = 1 - \frac{2\theta_1\theta_3}{3\theta_2^2}$$

Fault detection based on SPE can be performed

$$SPE \begin{cases} \leq SPE_\propto & fault\ free \\ > SPE_\alpha & fault \end{cases} \qquad (6.12)$$

Fault detection of multivariate systems using DPCA is comprised of off-line and on-line procedures and can be summarized as:

- The off-line procedure includes collecting the historical reference data and calculating the covariance matrix of the reference data. Several groups of reference data are organized into the time-lagged matrix form as in (6.2) and the average covariance matrix is calculated using equation (6.4) The numbers of principal component *a* and the matrices *P* and Λ are determined using the eigenvalue decomposition. The 95% control limit T_α^2 can be found by equation (6.7) and serves as the threshold setting.

- In the on-line monitoring, when a new measurement is available, the real-time T^2 is obtained using equation (6.6). If the value of real-time T^2 exceeds the 95% control limit T_α^2, it indicates that a fault occurs. Otherwise, no fault has occurred and the system is running normally. Fault detection can also be carried out similarly by calculating SPE as in (6.9).

The procedure of fault detection using DPCA and SPE are illustrated in Figure 16 and Figure 17.

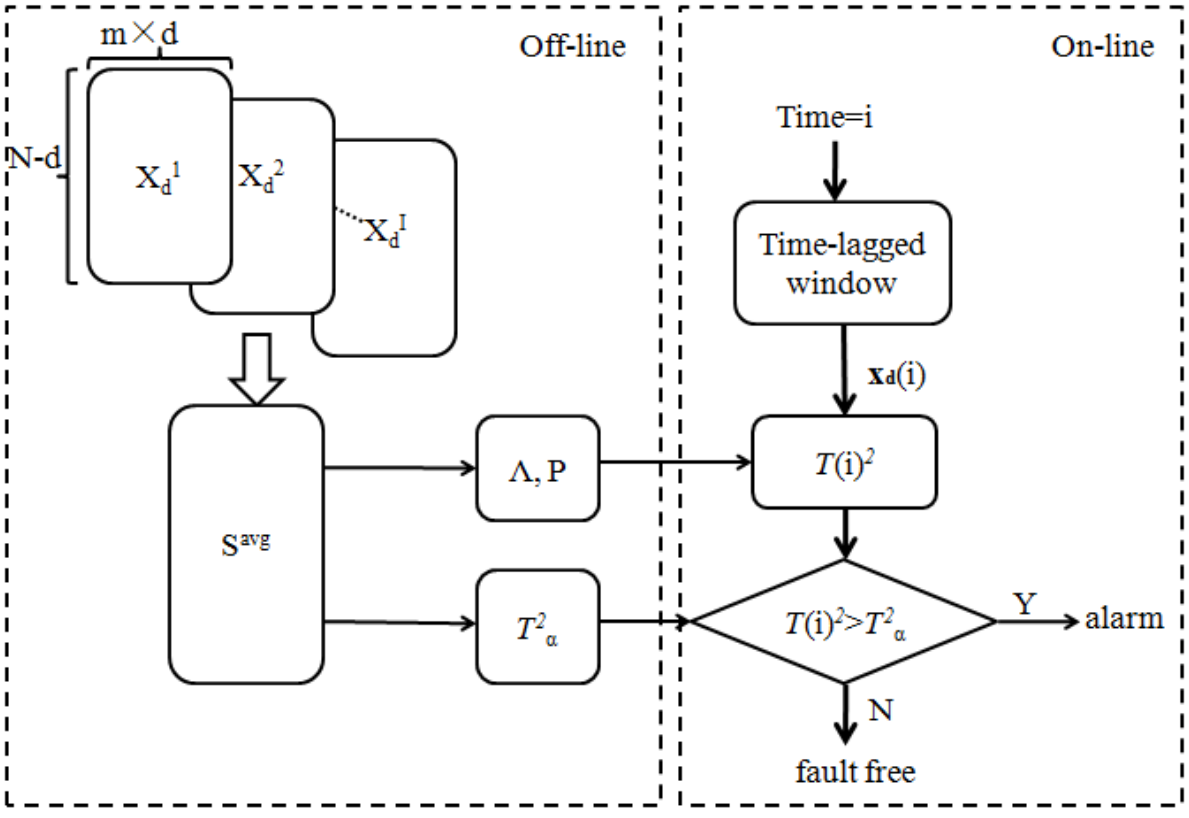

Figure 16: Fault detection procedure using DPCA

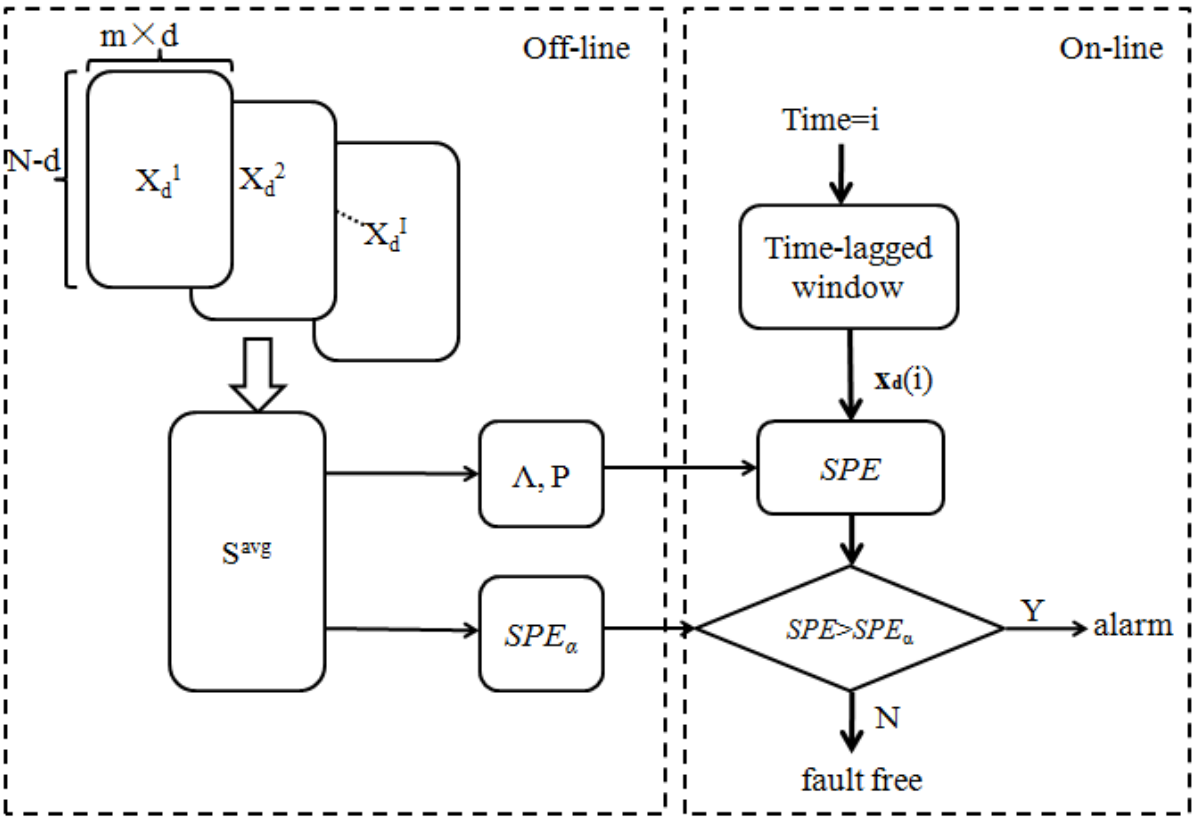

Figure 17: Fault detection procedure using SPE

6.2 Fault diagnosis using contribution plots

DPCA can be used to identify abnormality of a faulty process using statistical Hotelling's T^2. To further analyze the fault information, contribution plots are explored to examine the effect of each variable on the fault for the Se/Te removal and Cu electrowinning process. In the PCA based fault detection and diagnosis, the contribution plots decompose Hotelling's T^2 to components representing the contribution of individual process variables (He, et al., 2005; Guerfel, et al., 2009).

For the Se/Te removal and Cu electrowinning process, Hotelling's T^2 is obtained using the augmented variables with a time-lagged window. Based on the partial decomposition contribution method in obtaining the variable contributions for the conventional PCA (Alcala & Qin, 2011; Nomikos, 1997), a modified partial contribution decomposition is proposed to obtain the contributions of individual variables including the information over the time-lagged window. Define a column vector $\xi_k \in R^{md}$ for the k^{th} variable such that

$$\begin{aligned}
\xi_1 &= \left[1 \quad 0 \quad \dots \quad 0 \middle| 1 \quad 0 \quad \dots \quad 0 \middle| \dots \middle| 1 \quad 0 \quad \dots \quad 0\right]^T \\
\xi_2 &= \left[0 \quad 1 \quad \dots \quad 0 \middle| 0 \quad 1 \quad \dots \quad 0 \middle| \dots \middle| 0 \quad 1 \quad \dots \quad 0\right]^T \\
&\vdots \\
\xi_m &= \left[0 \quad 0 \quad \dots \quad 1 \middle| 0 \quad 0 \quad \dots \quad 1 \middle| \dots \middle| 0 \quad 0 \quad \dots \quad 1\right]^T
\end{aligned} \tag{6.13}$$

It can be obtained that the summation of $\xi\xi^T$ for all the variables is a unity matrix, i.e.,

$$\sum_{k=1}^{m} \xi_k \xi_k^T = I_{md \times md}$$

The contribution of the k^{th} variable at time t to Hotelling's T^2 can then be calculated as:

$$T^2_{contribution,k}(i) = \mathrm{x}_d(i)^T P \Lambda^{-1} P^T \xi_k \xi_k^T \mathrm{x}_d(i) \tag{6.14}$$

It is noted that even though $P\Lambda^{-1}P^T$ are positive semi definite, $P\Lambda^{-1}P^T\xi_k\xi_k{}^T$ may not be positive semi definite. The contribution from (6.14) may thus have negative values. In other words, a negative contributing variable does not necessarily mean it contributes less to the fault than a positive one or that the variable is decreasing inversely to the fault. With contributions of all variables obtained, the cause of abnormal operations can be analyzed and fault can be diagnosed by examining and comparing the relative contribution level of each variable.

6.3 Results and Discussion

To investigate the fault detection and diagnosis for the industrial Se/Te removal and Cu electrowinning process, one year's operating data have been examined. The 13 measurable variables are defined in the following table:

Table 2: Variables used in DPCA based fault detection

Variables	Description	Unit	Symbol
Variable 1	Temperature of electrowinning tankhouse feed	^oC	T1
Variable 2	Power rectifier voltage	Volts	V
Variable 3	Power rectifier current	Amps	I
Variable 4	Temperture of spent electrolyte	^oC	T2
Variable 5	Copper Concentration in spent electrolyte	g/L	$X2_{Cu}$
Variable 6	Feeding flow rate to the Se/Te removal circuit	L/min	F_f
Variable 7	Feeding temperature to the Se/Te removal circuit	^oC	T_f
Variable 8	Level in the Se/Te removal pump tank	%	L_{pump}
Variable 9	ORP measurement from #4 aging tower overflow	mV	ORP_{at}
Variable 10	Flow rate from underflow of #1 aging tower	L/min	F_{uf}
Variable 11	Glue addition rate	L/min	F_{glue}
Variable 12	Level in electrowinning mix tank	%	L_{ew}
Variable 13	Level in the return electrolyte tank	%	L_{spent}

A sampling time of 18 min was used in data collection. On preprocessing the measurements for fault detection, signal information for each variable was examined. It was noticed that there were missing measurements or unreasonable values (e.g., close to zero) for variable No.6. The measurement data for variable No.6 is preprocessed by replacing the missing or unreasonable data points with the estimate using average of the previous *n* measurements. In

applying DPCA, all the variables are normalized to the range of 0 to 1. Due to the operating condition of the copper electrowinning process, the measurements obtained from various field sensors may contain some noises. It is very important to preserve or enhance the signals while removing the noise for fault detection and diagnosis. In this work, due to relatively large sampling time (18 min) and data compression in recording industrial data, the information of high frequency noises no longer remains in the data and denoising was thus not applied.

The data was divided into 4 normal data sets and 3 faulty data sets based on the industrial product quality tests. A faulty data set refers to a time period that resulted in off-spec copper due to Se/Te contamination. From the normal data sets, the off-line reference data was established and the length of 2000 data points was used from each set. By setting the time lag window $d = 8$, the average reference covariance matrix S_{avg} for the augmented data matrix is obtained. The eigenvalues and eigenvectors for the covariance matrix S_{avg} are then calculated. The number of principal components a was set to 5, the eigenvalue Λ and eigenvector P corresponding to the 5 principal components can thus be found. Table 3 lists the parameter values used in the DPCA algorithm. Based on the reference data, the 95% control limit T_{α}^{2} is calculated to be 11.76.

Table 3: Parameter values used in the DPCA based fault detection and diagnosis

Parameter	Description	Value
d	Length of moving time lag window	8
a	Number of principal components	5
N	Length of each reference data set	2000
m	Number of variables	13
I	Number of reference data groups	4
α	Confidence level	95 %

The fault detection approach using DPCA was first applied to a new set of normal data with 2000 points. The real-time Hotelling's T^2 value is shown in Figure 18. It is observed that the Hotelling's T^2 values for all data points are below the control limit T_α^2.This indicates that no fault occurs and the fault detection result is consistent with the industrial tests for the normal operations.

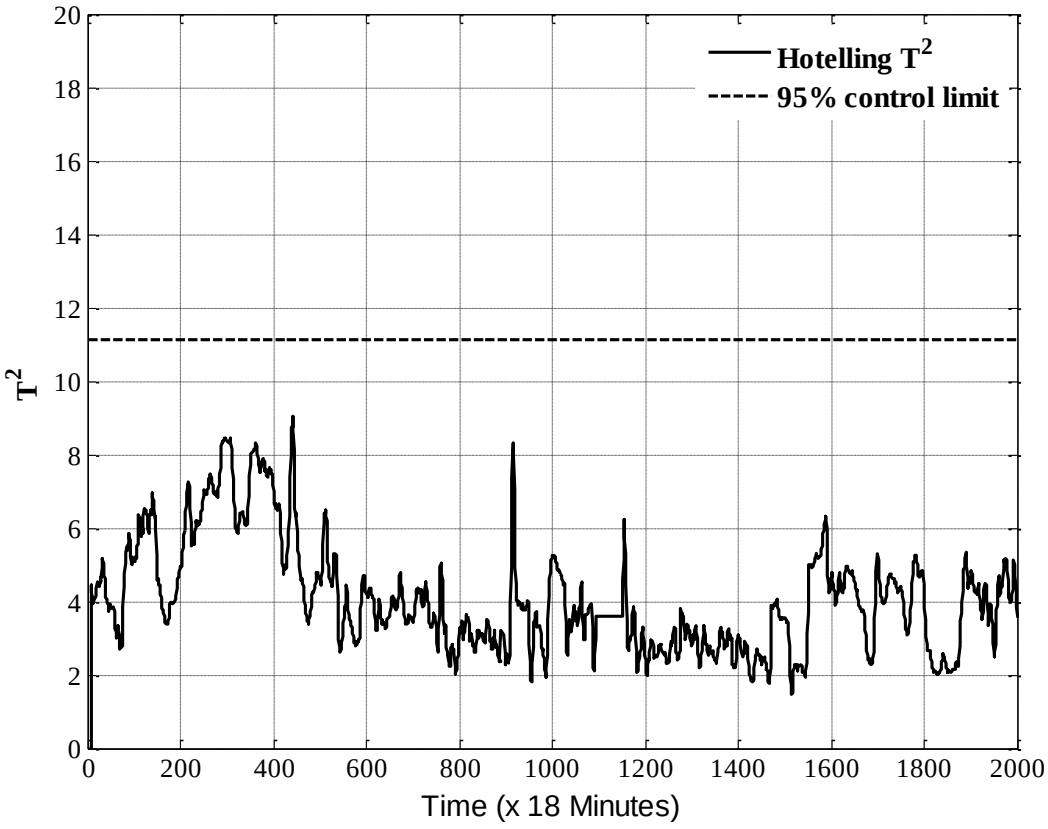

Figure 18: Hotelling's T^2 for a data set at normal operation

The normal data set was also analyzed using SPE, as in figure below. The SPE result is consistent with that using the Hotelling's T^2 and that all the values are below the control limit, indicating no fault in the operation.

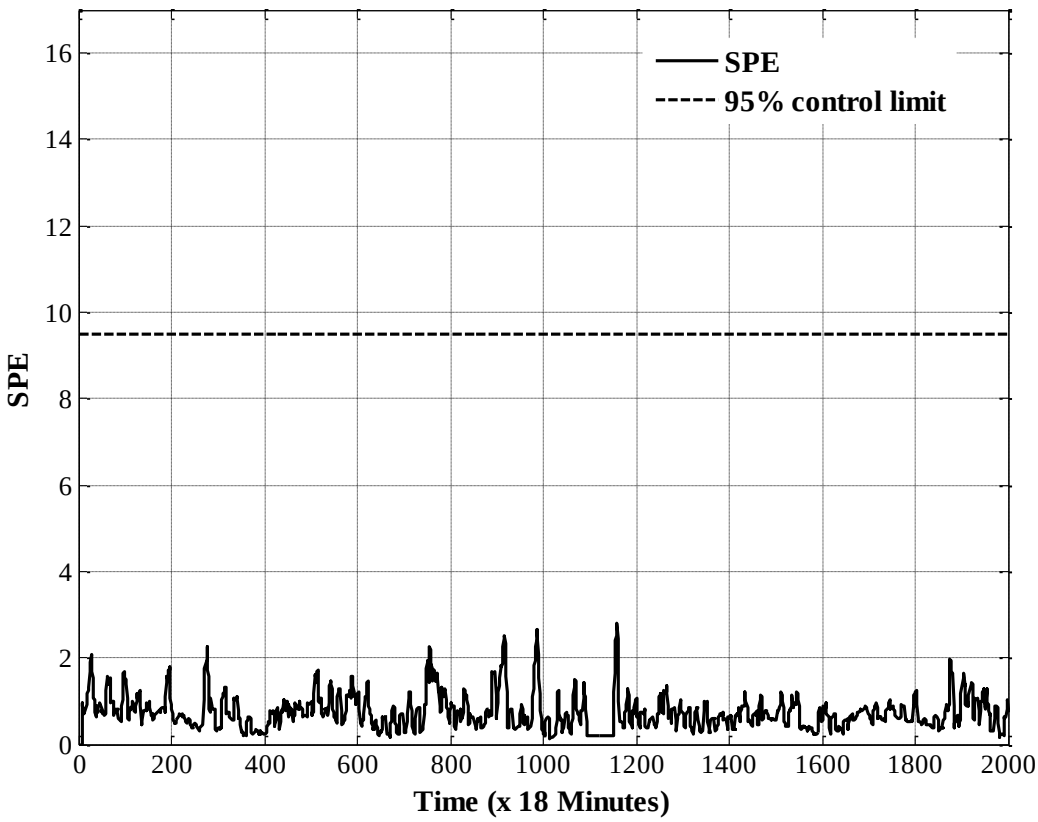

Figure 19: SPE for a data set at the normal operation

The faulty data sets are those when the product quality does not satisfy the specifications. The Se/Te removal and Cu electrowinning process has slow dynamics and it would be desirable to detect any faults from the operating data and to be able to determine the causes of the faults from the data. Three faulty data sets, listed in Table 4, were collected from the industrial system and examined using the DPCA based fault detection and diagnosis.

Table 4: Faulty data sets tested for fault detection and diagnosis

Test Sample No.	Length
Run-1	2881
Run-2	3601
Run-3	4324

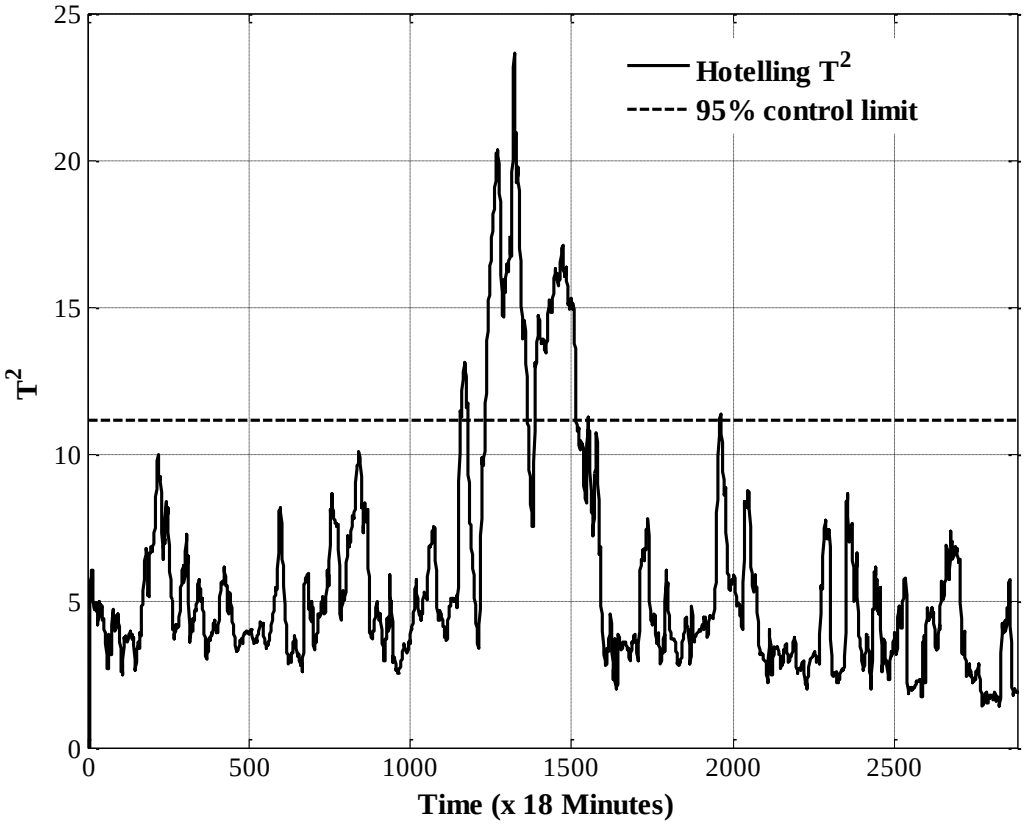

Figure 20: Hotelling's T^2 for the faulty data set Run No.1

shows the Hotelling's T^2 when the DPCA based fault detection is applied to the faulty data Run No.1. It is observed that the control limit is violated at t = 1235 indicating that a fault occurred at this time. The Hotelling's T^2 statistic shows that the process experienced a sustained fault, which indicates it was not merely noise or disturbance. The faulty operation sustained until t = 1514.

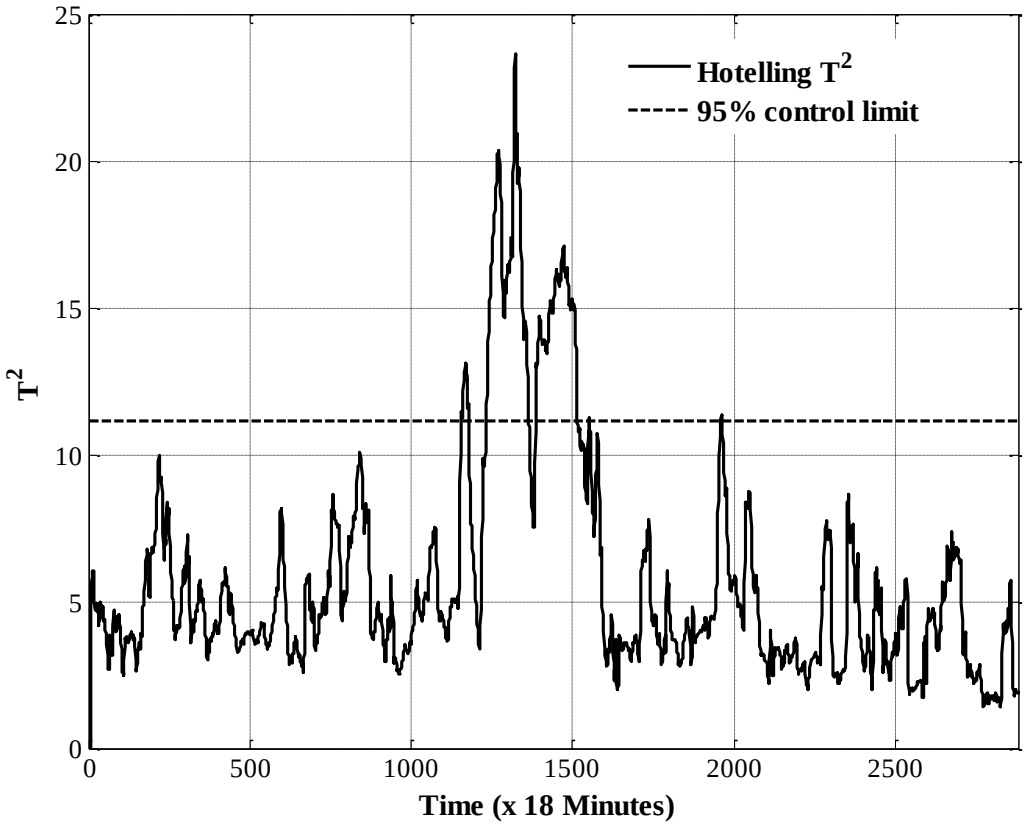

Figure 20: Hotelling's T^2 for the faulty data set Run No.1

SPE values are obtained for the faulty data Run No.1, as shown in Figure 21. It confirms that a fault occurred for the operation. Comparison of Figure 20 and Figure 21 indicates that similar results are generated using both fault detection approaches. The period of violation

according to SPE appears to be shorter than using the Hotelling's T^2 statistic. The difference may be due to a trade-off between sensitivity and robustness of the two methods. Although the remaining time period is below the 95% control limit, the Hotelling's T^2 statistic overall appears more noisy making it more sensitive to predicting upset conditions. On the down side, a highly sensitive fault detection method could incorrectly predict a fault when none occurred. Alternatively, SPE fault detection seems more robust but could potentially have the downfall of missing a fault altogether.

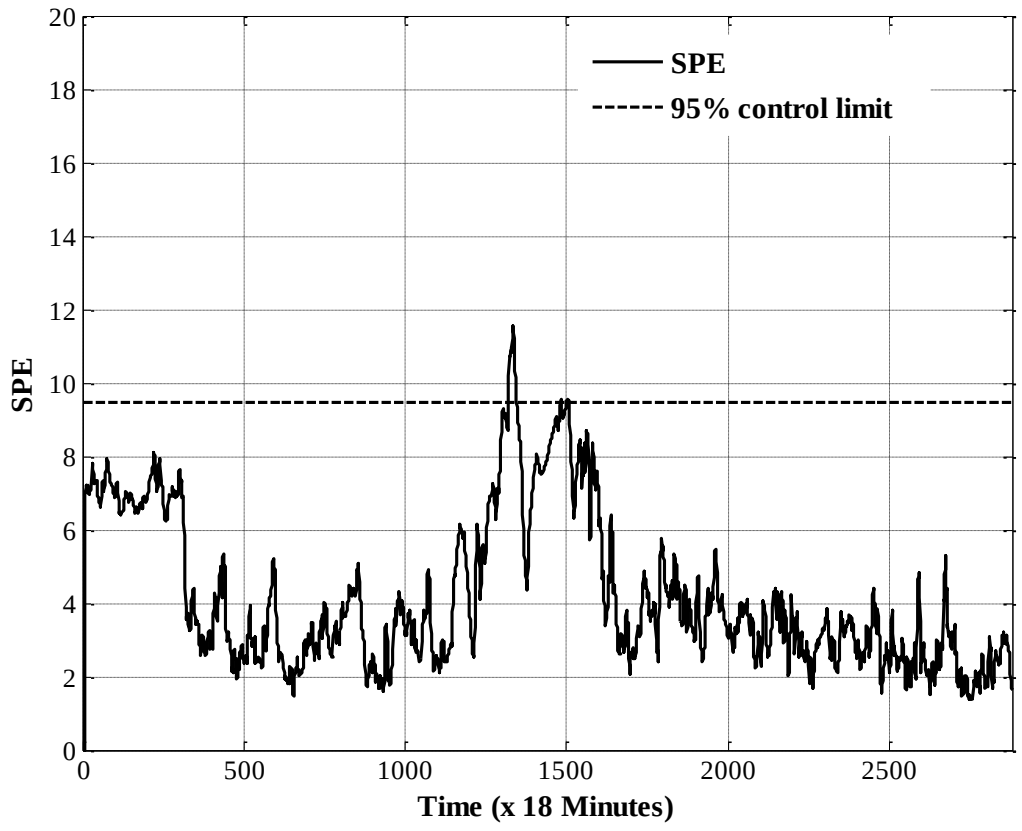

Figure 21: SPE for the faulty data set Run No.1

The contribution of individual variables to the fault is investigated by examining the contribution plot for the data when Hotelling's T^2 violates the control limit T_α^2. The contribution plot at t = 1244 is obtained as in Figure 22.

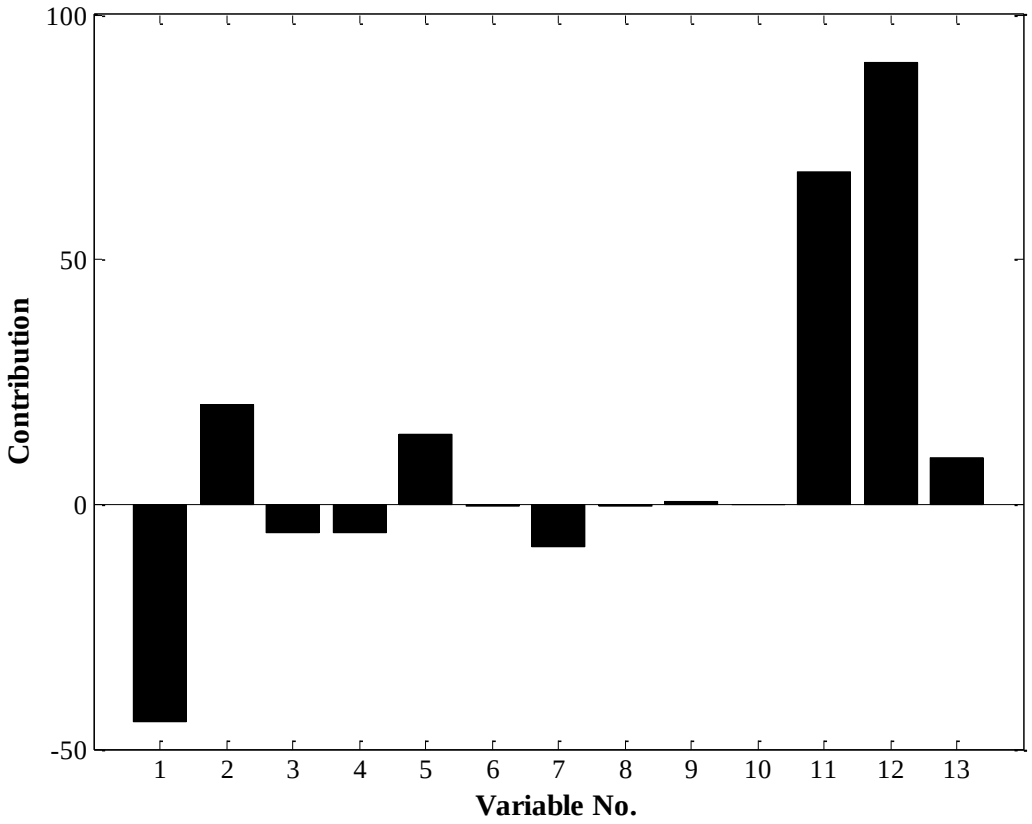

Figure 22: Contribution plot for the faulty data set Run No.1 at t=1244

It demonstrates the contribution plot for a faulty data set that resulted in the production of high Te content in copper cathodes (>5 ppm Te). The main variables that appear to contribute significantly to this upset include the temperature of tankhouse feed (variable 1), glue addition rate (variable 11) and level in the Electrowinning Mix Tank (variable 12). Tankhouse feed temperature is an important parameter to ensure optimum electrolyte

conductivity in the tankhouse. A lower temperature could also result in the formation of copper sulphate crystals which in turn increases the chance of plugging or disrupting flows and ultimately causing plating issues. Upon further analysis of this time period, there were reports of “bluestone” (copper sulphate crystals) build-up around the inlet of electrowinning cells which could have formed as a result of low tankhouse feed temperature. In this faulty data set, glue addition rate was also named as a high contributing factor. Glue addition acts as a leveling agent to help form smooth nodule-free copper cathodes. Consequently, if too much glue is added it can form rounded nodules on the cathode or needle like nodules if not enough is added to the electrolyte. Further review of data indicated that there was actually an instrumentation failure during this time, displaying a faulty reading of glue addition. If glue addition was removed as a variable from the DPCA, this would most likely alter the contribution plot and divert the emphasis of the contribution to a different variable. Finally, the Electrowinning Mix Tank level represents the strongest contribution inclusively. Operating at peak capacity, in this case at 100% of level capacity, can only be sustained for so long before it effects equipment, solution handling and overall product quality. Investigation into this time period revealed a continuous two week stunt at 100% level capacity.

DPCA based fault detection and diagnosis was carried out for the faulty data Run No.2 and Figure 23 shows the Hotelling's T^2 for the data. For this data set, Hotelling's T^2 appears different from that for Run No.1. It violates the control limit T_α^2 at several data ranges and

each violation is not as sustained and substantial as that for Run No.1. The notable violations mainly occur between t = 2700 and t = 2900.

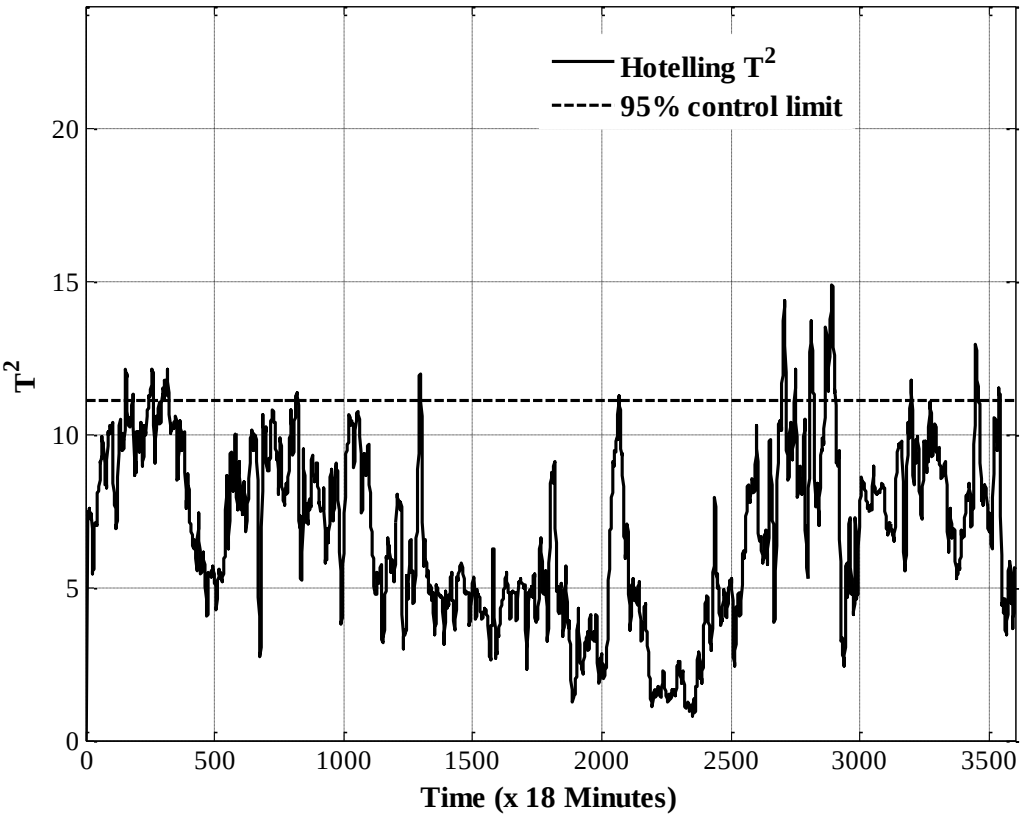

Figure 23: Hotelling's T^2 for the faulty data set Run No.2

The SPE result, as in Figure 24, shows a short and insignificant violation in SPE, implying that the abnormality for the faulty data Run No.2 may not be substantial.

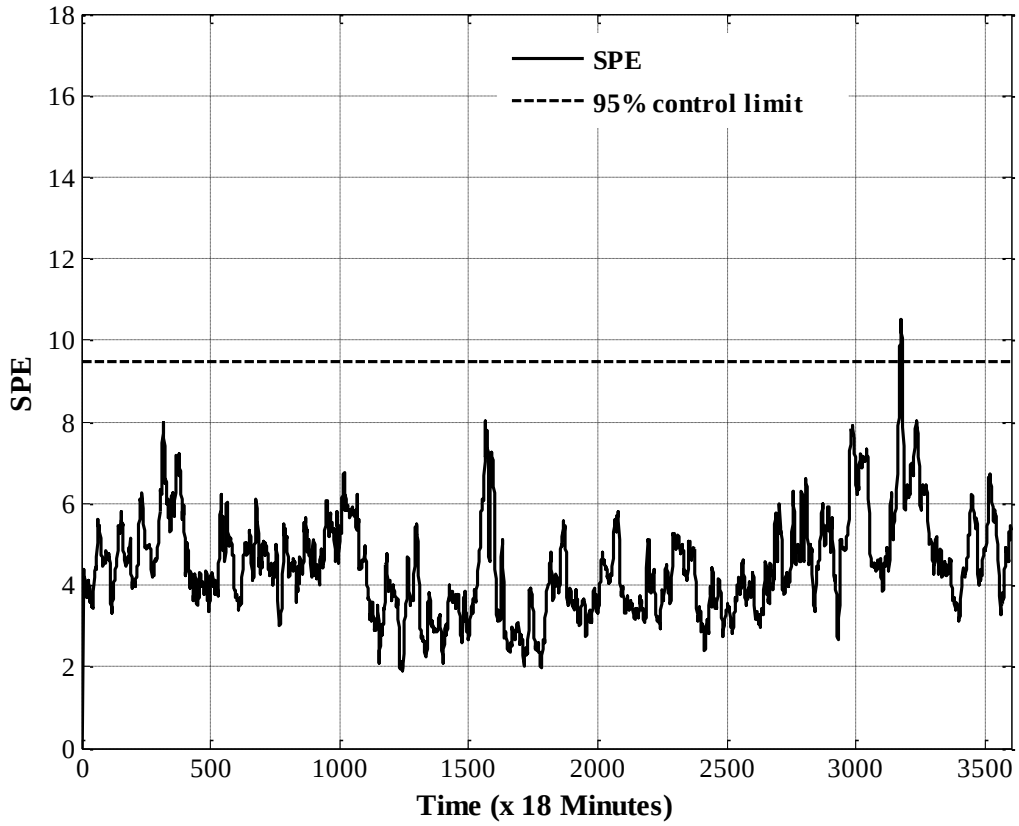

Figure 24: SPE for the faulty data set Run No.2

For fault detection, the Hotelling's T^2 can be calculated based on either PCA or DPCA. Conventionally PCA has been widely accepted in many applications due to computational simplicity and DPCA is an extension of the conventional PCA and usually requires more demanding computation depending on the chosen time lag of the data in (6.2). To compare performance of the fault detection methods based on DPCA and conventional PCA for the Se/Te removal and Cu electrowinning process, the Hotelling's T^2 based on PCA is calculated for the faulty data Run No.2. From Figure 25, it is observed that almost all the data points are within the control limit for the faulty operation. The result indicates that the conventional

PCA based Hotelling's T^2 fails to detect the fault in the data Run No.2 while the DPCA based approach can successfully detect it. PCA based fault detection was also examined on other faulty data sets. It is found that it is able to detect faults when substantial faults occur, e.g., in the faulty data Run No.1, but has difficulty when abnormity is less obvious as in the faulty data Run No.2. This confirms that DPCA based fault detection is a preferred choice for the Se/Te removal and Cu electrowinning process due to the slow and complicated system dynamics.

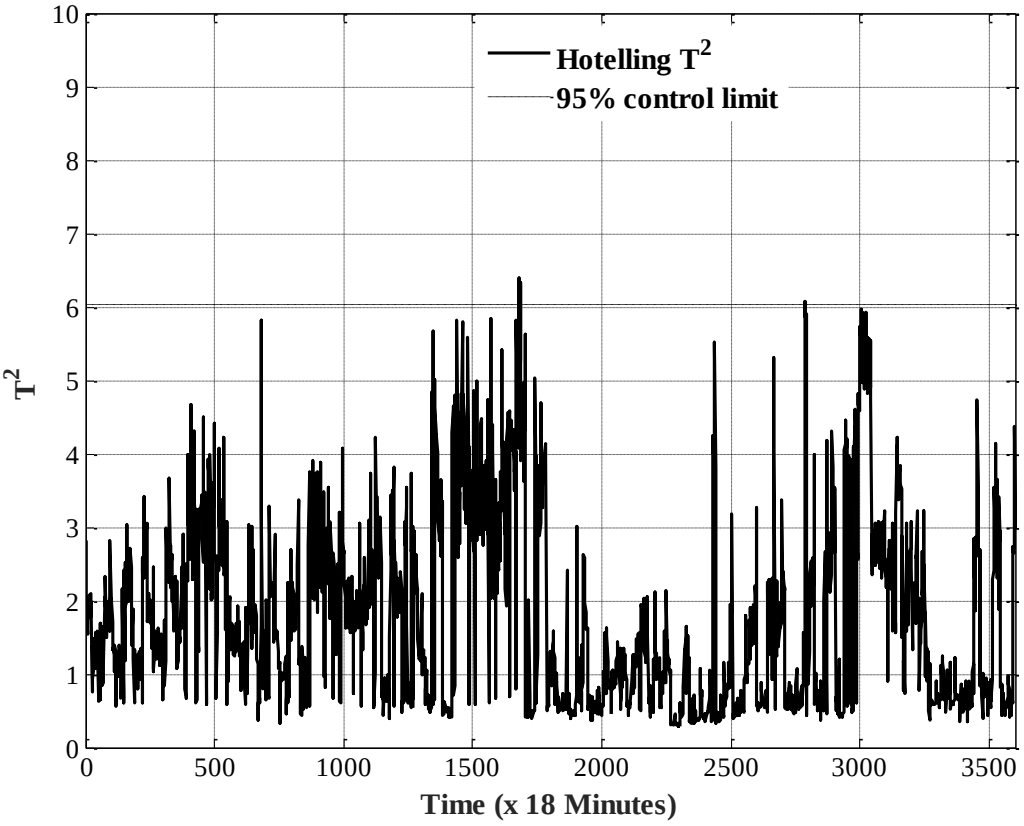

Figure 25: PCA based Hotelling's T^2 for the faulty data set run No.2

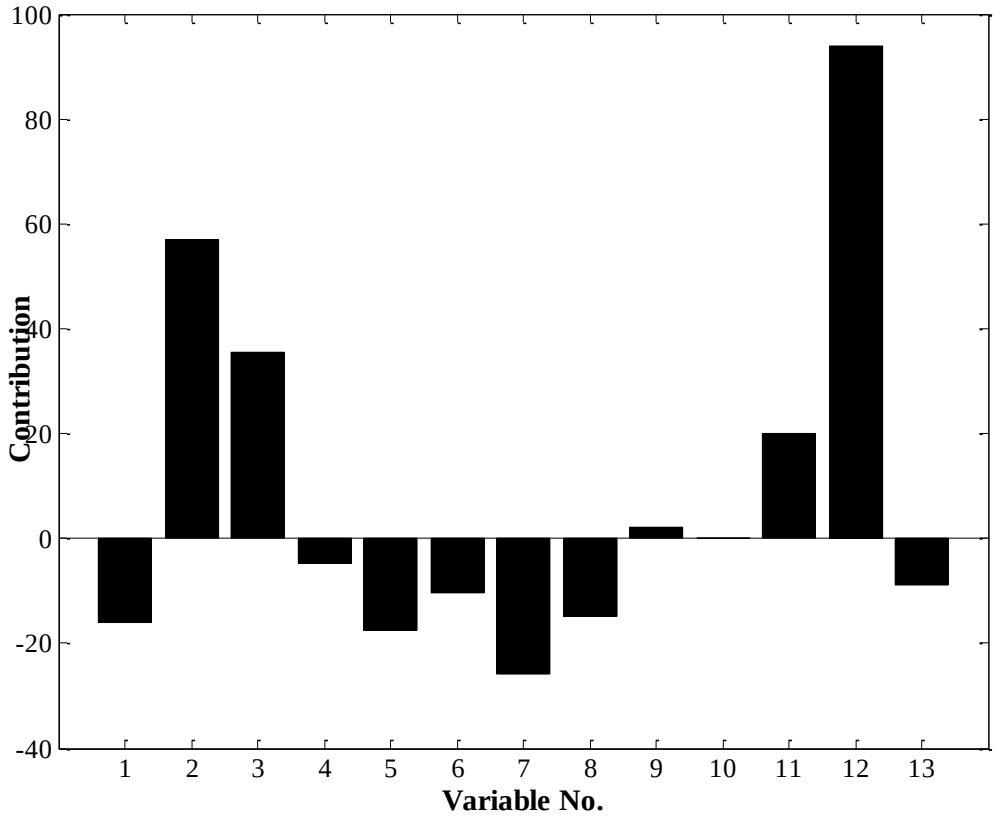

Figure 26: Contribution plot on faulty data set Run No.2 at t=2702

To analyze the possible causes for the fault, the contribution plot at t = 2702 is obtained as in Figure 26. It reveals a slightly different faulty data set with power rectifier voltage, power rectifier current and level in the Electrowinning Mix Tank being the most dominant contributors. Similarly to the first upset condition, the electrowinning tank was operating near 100% for an extended period of time. When operating near capacity, electrolyte begins to overflow from the Electrowinning Mix Tank to the basement of the tankhouse. This, unfortunately, allows the basement electrolyte to be continuously exposed to oxygen which can reverse Te precipitation reaction and in turn cause the Te to go back into solution. So

eventually when the basement electrolyte is reprocessed to the front of the Se/Te Removal Circuit, the amount of Te can be beyond the capacity of the Cu Shot Column to handle, leaving high Te in electrolyte to be plated out in the tankhouse. Reports of significant increase in basement electrolyte handling during this time period further supports this conclusion. A lower power rectifier voltage and current may compound this issue further. If Te is already high in electrolyte, lowering the voltage and current means less Cu is plating out causing the off-spec production to be extended. Analyzing the data in more detail from this time period, the voltage and current were very erratic but generally lower than typical operation for two weeks. Furthermore, there were several reports of low copper in spent, acid misting and rectifier issues during this period.

For the faulty data Run No.3, DPCA was applied and the Hotelling's T^2 is obtained as in Figure 27. It is noticed that the $T^2(j)$ statistic violates the control limit at t = 192 and t = 2113. These two violations quickly disappear in the next time lag window. They may be caused by noise or disturbance and can be neglected. A sustained violation occurs from t = 3396 to t = 3503, indicating that a fault occurred during this period of time.

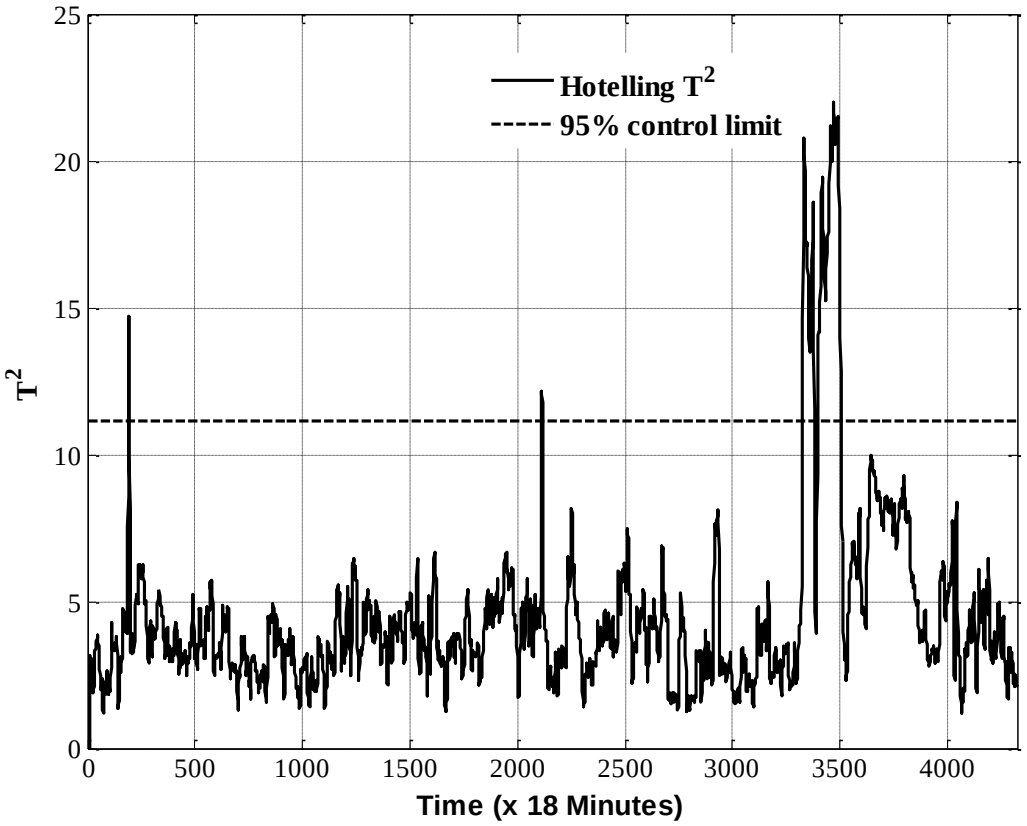

Figure 27: Hotelling's T^2 for the faulty data set Run No.3

Figure 28 shows SPE for the faulty data Run No.3 and it can be seen that consistent fault detection is obtained using both the Hotelling's T^2 and SPE. The short and negligible violations in the Hotelling's T^2 at t = 192 and t = 2113 do not appear in the SPE test. This is most likely a result of SPE being less sensitive to smaller fluctuations in the process that may lead to a fault.

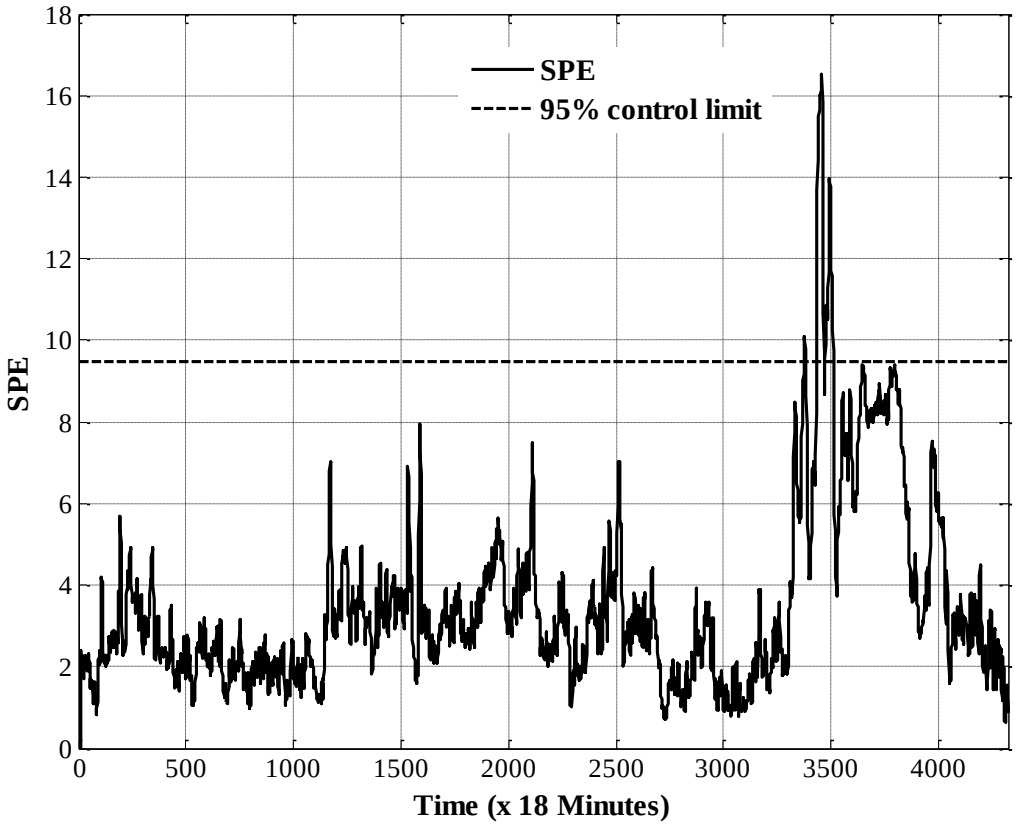

Figure 28: SPE for the faulty data set Run No.3

The contribution plot at t = 3405 is obtained as in Figure 29. The upset in Figure 29 is very different as there are multiple contributors. Variables 1, 2, 3, 5 and 7 appear to contribute the most to this upset though not as much as the other two, with contribution only slightly greater than 10. These variables represent temperature of tankhouse feed, power rectifier voltage, power rectifier current, copper concentration in spent electrolyte and feeding temperature to Se/Te Removal Circuit. Further analysis into the data revealed that most of these variables fluctuated as a result of two down days during this two month period. The down days were

the effect of an upset condition not necessarily the cause that resulted in off-spec copper production.

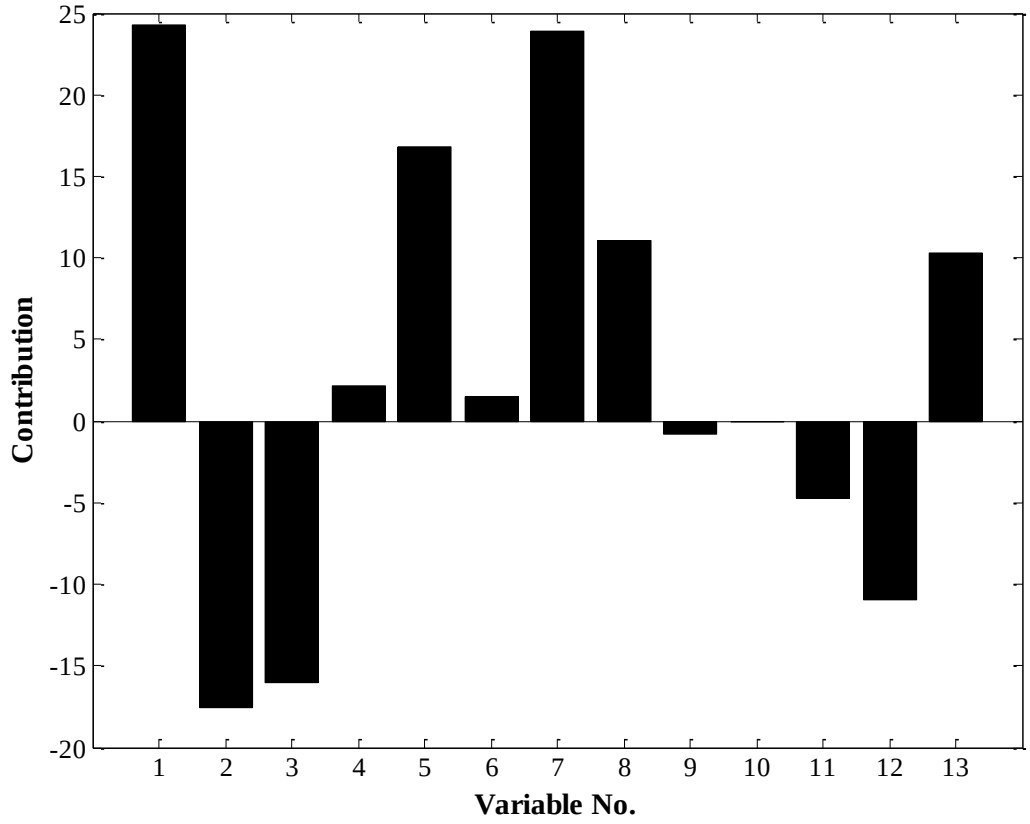

Figure 29: Contribution plot on faulty data set Run No.3 at t=3405

The DPCA based fault detection was applied to three faulty data sets and all the faults were detected effectively. This shows that the DPCA based fault detection is valid for the industrial Se/Te removal and Cu electrowinning process. In the existing industrial practice, the faults can be detected when the final products are produced and tested, which could be many days later after occurrence of faults. DPCA based fault detection can detect the faults based on online operating measurement and can, therefore, be used in quickly correcting the

faulty operation. From the analysis of the contribution plots for three faulty data sets, the contribution plots did provide merit in determining actual potential causes of off-spec production, especially when the contribution level was greater than 25. The advantage of these contribution plots is that it enables sorting of numerous variables to help narrow down potential causes of an upset condition. On the down side, the contribution plot is only as good as your data as it assumes the data is reliable and representative of actual events. Furthermore, the contribution plots can develop as a better predictive tool as more variables become measurable. These faulty data sets utilized 13 variables but there are numerous others that could come into play, such as pump speed, pressure indication, more flow indicators, etc., and alter the level of contribution. In the mean time, applying the fault detection to historical data may help to build a database of faults and further validate this DPCA method to the electrowinning process.

Accuracy is an important factor in fault detection and diagnosis. Accuracy of fault detection is affected by the set confidence level α. In this work, the confidence level is set as $\alpha = 95\%$, implying 5% allowable false alarm rate. It is desirable to have reduced false alarm rate, which can be achieved by increasing the confidence level α. Higher α, however, leads to higher missing report rate. For the work in this paper, one year's operating data was analyzed and, among the collected data, only three periods of faulty operations were confirmed based on industrial product quality tests. For the three faulty data sets, the DPCA based fault detection approach is able to successfully detect faults, and the results are consistent with the industrial quality tests. Due to the limitation of faulty samples, a full assessment of fault

detection accuracy cannot be formed from the limited faulty samples. In the future work, it is essential to establish a mechanism to assess the false alarm rate and missing report rate by building a larger database for various faulty operations.

6.4 Conclusions

In this chapter, fault detection and diagnosis for the industrial Se/Te removal and Cu electrowinning process is investigated using the DPCA based approach. The Se/Te removal and Cu electrowinning process has slow dynamics with long residence time. DPCA establish a time-lagged moving window to contain more information of process variables which can reflect the correlation of different variables in different time. For the variables augmented with the time lag window, DPCA is used to derive the principal components of reduced dimension. The Hotelling's T^2 and SPE are then calculated and used for fault detection. The detection results based on the operating data matches with the industrial product quality tests. It is concluded that the DPCA based fault detection is effective for the industrial Se/Te removal and Cu electrowinning process

After a fault is detected, the fault can be diagnosed for possible causes. A modified partial decomposition contribution is proposed to calculate the contribution of variables to the Hotelling's T^2 and applied to the fault diagnosis of the industrial Se/Te removal and Cu electrowinning process. The contributing variables obtained from the fault diagnosis is compared and confirmed with industrial reports during the faulty periods. It indicates that the contribution plots provide an indication for the possible causes of the faults when

measurement is reliable. Further diagnosis of root causes can be achieved by building a database on all kinds of faults and the root causes related to the faults.

Chapter 7: Conclusions and Recommendations

7.1 Summary of Dissertation Results and Conclusions

The focus of the dissertation was to deliver a model that is able to simulate key parameters of an actual copper electrowinning process. Dynamic models of the copper concentration and temperature in the electrowinning tankhouse have been developed. These models are based on fundamental principles of mass and energy conservation laws as well as Faraday's Law. The resultant PDEs take the form of first order hyperbolic, only when the effect of diffusion is considered negligible. As such, these first order hyperbolic PDEs are sufficient in relating variations of copper concentration and temperature. When comparing the actual industrial data, there is a reasonably good fit to the predicted data from these models. The developed models may provide a means to further understand variability in the process under different operating conditions.

Furthermore, a fault detection method using all available process data was applied from the Se/Te removal and copper electrowinning circuits. The purpose of the fault detection is to pinpoint the key process variables that lead to upset conditions in the circuits. Based on dynamic principal component analysis (DPCA), T^2 value and SPE are computed and used to detect whether a fault occurred. In comparing the two methods, Hotelling's T2 appears to be a more sensitive means of predicting a fault. DPCA based fault detection is more fitting than

other methods, due to the time lagged information, to produce a dependable fault detection of a time transient electrowinning system. Three faulty data sets were collected from the provided process data, based on the time period that resulted in off-spec Cu production. Upon identifying key contributions to each fault, the contribution of all 13 variables was interpreted on the possible impact to how it may have added to off-spec Cu production. The 13 variables are all the measureable variables available from the actual plant process. Although the main contributors may change from fault-to-fault due to the complexity of the circuits and chemistry involved, the Electrowinning Mix Tank level appeared to be a consistent and likely contributor to a fault. If the level of the tank feeding the electrowinning circuit is steadily overflowing beyond capacity, the excess electrolyte is sent to the tankhouse basement until it can be reprocessed. Unfortunately, this allows for the electrolyte to be cooled and oxidized which in turn can cause Te to redissolve back into solution and overwhelm the Se/Te circuit upon reprocessing. When it comes to a trade-off between sensitivity and robustness of the prediction, it is preferable to incorrectly predict a fault than to miss the fault entirely making DPCA a better fit than SPE for this application. Overall results concluded that the DPCA based fault detection and diagnosis is an effective method for highlighting the contributions to the faults that arise in the Se/Te removal and Cu electrowinning process.

7.2 Recommendations for Future Work

Currently, there are only two ways to monitor the performance of the Se/Te Removal Circuit: online ORP measurement and sample analysis. The ORP (Oxidation Reduction Potential) measurement indirectly indicates how much Se and Te have been removed from solution. For

example, if the ORP is reading less than 160 mV then most of the Se and Te have been reduced and precipitated to a solid form. As the ORP starts to rise above 160 mV this would indicate a potential upset, leaving excessive Se and Te in solution. The disadvantage of this measurement is that it does not provide how much Se and Te actually remain in solution. Therefore, a grab and composite sample is taken from the #4 Aging Tower overflow and the return electrolyte tank to capture the quantity of Se and Te before and after the electrowinning process. Sample analysis becomes very important then to help predict how much Se and Te will be plated and the extent of the upset. Unfortunately, sample preparation and analysis is cumbersome and can only be realistically provided on a daily basis. Estimating Se and Te concentrations at a higher frequency rate could greatly improve this prediction and perhaps allow a quicker response to take action to try and reduce the overall upset. Future work should involve extending a similar model in Chapter 5 on Cu concentration to predicting Se and Te concentrations in spent electrolyte.

In terms of fault detection improvements, a collection or database of faults with associated root causes should be formed to ease the diagnosis and intervention process to eliminate the fault. A continuous collection and database should be fairly easy to set-up at the electrowinning plant as the variables utilized in this fault detection work are already continuously measured. The off-line algorithms (as shown in Figure 13) to calculate the Hotelling's T2 value should be run on an hourly frequency to ensure a fault could quickly be detected and corrected. A database of faults will also help to determine which variables contribute little to nothing to the faults and in turn be eliminated as a potential cause. This

would serve to better improve the accuracy of the contribution level of each remaining variable. Furthermore, as new measurable variables around the circuits become available they should be incorporated into the DPCA based fault detection. DPCA ability to predict a fault is only as good as the data and measurable variables that it can collect. The likelihood of predicting a fault and actual contributors will then improve accordingly.

Nomenclature

Below is a list of all variables and parameters used throughout the dissertation.

Notation	**Description**
ϕ_i	current efficiency of species *i* [%]
P_i	Rate of metal deposition of species *i* [g/min]
M_i	molecular weight of species *I* [g/mol]
I	Electrical current [Amps]
F	Faraday's Law [Coulombs]
Z_i	number of electrons involved in reaction
x	variable vector
m	number of variables
S	Covariance matrix of x
p_k	Eigenvector of S with the k^{th} largest eigenvalue
λ_k	k^{th} largest eigenvalue
t_k	The k^{th} principal component
e	residual matrix
V	Volume of the electrolyte [g/m^3]
A	Cross-sectional area of the cell [m^2]
u	Flow speed through the cell [m/min]
X_{Cu}	Copper concentration [g/m^3]
Δz	Distance between node *i* to node *i+1* [m]
Δt	Time difference between node *i* to node *i+1* [min]
P	Rate of copper deposition [g/min]
M_{Cu}	Molecular weight of Cu [g/mol]
Z	Number of electrons involved in copper deposition reaction

ϕ	current efficiency of copper to deposit on cathodes [%]
t_R	residence time [min]
D	diffusivity coefficient of copper in solution [m^2/min]
Q	Flow rate of electrolyte [m^3/min]
T	Electrolyte temperature [^oC]
ρ	density of electrolyte [g/m^3]
c_p	Specific heat coefficient
R	resistance
D_T	Thermal diffusivity coefficient [m^2/min]
d	previous observations
i	current time constant [min]
N	number of observations
X_d	data matrix with previous d observations
S_j	covariance matrix corresponding to the j^{th} group
S^{avg}	average value of the covariance matrix S
p_j	Eigenvector corresponding to the j^{th} largest eigenvalue
λ_j	the j^{th} largest eigenvalue
t_j	the j^{th} principal component
Λ	diagonal matrix containing the largest eigenvalues
a	the largest eigenvalues
P	loading vectors associated with the a largest eigenvalues
$F_{a, K\text{-}d\text{-}a,\alpha}$	the F-distribution above the critical point α with a and $N - d - a$ degrees of freedom
r	The residual vector
N_α	normal distribution with confidence limit α
α	the confidence level which is generally set as 95%

ξ_k a column vector for the k^{th} variable

Table of Acronyms

Below is a list of all acronyms used throughout the dissertation.

Notation	**Description**
DPCA	dynamic principal component analysis
DC	direct current
SX	solvent extraction
EW	electrowinning
ODE	ordinary differential equation
PDE	partial differential equation
SPC	statistical process control
PCA	principal component analysis
PC	principal component
IPC	Inco pressure carbonyl
SAG	semi autogenous grinding
TBRC	top blown rotary converter
SPE	squared prediction error

Works Cited

Alcala, C. F. & Qin, S. J., 2011. Analysis and generalization of fault diagnosis methods for process monitoring. *Journal of Process Control,* 21(3), pp. 322-330.

Aminian, H., Bazin, C., Hodouin, D. & Jacob, C., 2000. Simulation of a SX-EW pilot plant. *Hydrometallurgy,* 56(1), pp. 13-31.

Beukes, N. T. & Badenhorst, J., 2009. Copper electrowinning: theoretical and practical design. *The Journal of The Southern African Institute of Mining and Metallurgy,* Volume 109, pp. 343-356.

Carr, H., Humphris, M. J. & Longo, A., 1997. *The Smelting of Bulk CuNi Concentrates at the Inco Copper Cliff Smelter*. Sudbury, Proceedings of the Nickel-Cobalt 97 Internatiional Symposium, Volume 3, 5-24.

Chen, J. & Liu, K. C., 2002. On-line batch process monitoring using dynamic PCA and dynamic PLS. *Chemical Engineering Science,* 57(1), pp. 63-75.

Clark, R. N., 1979. *The dedicated observer approach to instrument fault detection.* Fort Lauderdale, FL, 18th IEEE Conference, Volume 2, 237-241..

Cramb, A. W., 2005. *A Short History of Metals.* [Online]
Available at: http://neon.mems.cmu.edu/cramb/Processing/history.html
[Accessed 13 June 2015].

Davenport, W. G., King, M., Schlesinger, M. & Biswas, A. K., 2002. *Extractive Metallurgy of Copper*. Kingston, Oxford, UK: Elsevier Science Ltd.

Ding, S., 2013. *Model-based Fault Diagnosis Techniques, Design Schemes, Algorithms and Tools,* London: Springer.

Donald, J. R. & Scholey, K., 2005. *An Overview of Inco's Copper Cliff Operations,* Copper Cliff, ON: Vale Canada Ltd..

Frank, P. M., 1990. Fault diagnosis in dynamic systems using analytical and knowledge based redundancy: a survey and some new results. *Automatica,* 26(3), pp. 459-474.

Gentil, S., Lesecq, S. & Barraud, A., 2009. Improving decision making in fault detection and isolation using model validity. *Engineering Application of Artifical Intelligence,* Volume 22, pp. 534-545.

Guerfel, M., Aicha, A. B., Othman, K. B. & Benrejeb, M., 2009. *An improved principal component analysis scheme for sensor fault detection and isolation: Application to a three tanks system.* Makedonia Palace, Thessaloniki, Greece, Control and Automation, 17th Mediterranean Conference.

He, Q. P., Qin, S. J. & Wang, J., 2005. A new fault diagnosis method using fault direction in fisher discriminant analysis. *AIChE Journal,* 51(2), pp. 555-571.

Himmelblau, D., 1978. *Fault Detection and Diagnosis in Chemical and Petrochemical Processes,* Amsterdam: Elsevier Press.

Hinatsul, J. T. & Foulkes, F. R., 1989. Diffusion coefficients of copper (II) in aqueous cupric sulfate-sulfuric acid solutions. *Journal of the Electrochemical Society,* 136(1), pp. 125-132.

Hoffman, J. E., 1989. Recovering Selenium and Tellurium from Copper Refinery Slimes. *JOM, Volume 41, Issue 7,* pp. 33-38.

Jackson, J. E., 1991. *A User's Guide to Principal Components.* New York: Wiley.

Khouraibchia, Y., 2009. *Improving the Fundamental Understanding of Copper Electrowinning,* Utah: The University of Utah.

Kourti, T. & MacGregor, J. F., 1996. Multivariate SPC methods for process and product monitoring. *Journal of Quality Technology,* Volume 28, pp. 409-428.

Ku, W., Storer, R. H. & Georgakis, C., 1995. Disturbance detection and isolation by dynamic principal component analysis. *Chemometrics and Intelligent Laboratory Systems,* Volume 30, pp. 179-196.

Lee, J., Yoo, C. & Lee, I., 2004. Fault detection of batch processes using multiway kernel principal component analysis. *Computers & Chemical Engineering,* 28(9), pp. 1837-1847.

Lesecq, S. & Gentil, S., 2008. Signal-based diagnostic algorithms integrating model validity in the decision. *Control Engineering Practice,* 16(9), pp. 1120-1131.

Lie, B. & Hauge, T. A., 2008. *Modeling of an industrial copper leaching and electrowinning process with validation against experimental data.* Norway, Proceedings SIMS 2008, 49th Scandinavian Conference on Simulation and Modeling..

Li, G., Qin, S. J. & Chai, T., 2014. *Multi-directional reconstruction based contributions for root-cause diagnosis of dynamic processes.* Portland, OR, American Control Conference, 3500-3505.

Massoumnia, M. A., 1986. A geometric approach to the synthesis of failure detection filters. *IEEE Transaction on Automatic Control,* 31(9), pp. 839-846.

Mehranbod, N., Soroush, M. & Panjapornpon, C., 2005. A method of sensor fault detection and identification. *Journal of Process Control,* 15(3), pp. 321-339.

Mokmeli, M., Dreisinger, D. B. & Wassink, B., 2014. *Fundamental Studies in Selenium and tellurium Removal from copper Sulfate-Sulfuric Acid Solutions with Application to Industrial Purification,* Vancouver, BC: University of British Columbia, Department of Materials Engineering.

Nimmo, I., 1995. Adequately address abnormal situation operations. *Chemical Engineering Progress,* 91(9), pp. 36-45.

Nomikos, P., 1997. *Statistical monitoring of batch processes, in: Preprints of Joint Statistical Meeting,* Anaheim, CA: s.n.

Power, Y. & Bahri, P. A., 2004. A two-step supervisory fault diagnosis framework. *Computers & Chemical Engineering,* 28(11), pp. 2131-2140.

Quickenden, T. I. & Jiang, X., 1984. The diffusion coefficient of copper sulphate in aqueous solution. *Electrochimica Acta,* 29(6), pp. 693-700.

Rao, G. S., Gokhale, Y. W. & Gupta, S. S., 1976. Recovery of Selenium & Tellurium from Anode Slimes. Volume 14, pp. 201-203.

Ruiz, D. et al., 2000. Neural network based framework for fault diagnosis in batch chemical plants. *Computers & Chemical Engineering,* Volume 24, pp. 777-784.

Russell, E. L., Chiang, L. H. & Braatz, R. D., 2000. *Data-Driven Methods for Fault Detection and Diagnosis in Chemical Processes,* Springer-Verlag, London: s.n.

Russell, E. L., Chiang, L. H. & Braatz, R. D., 2006. Fault detection in industrial processes using canonical variate analysis and dynamic principal component analysis. *Chemometrics and Intelligent Laboratory Systems,* Volume 51, pp. 81-93.

Sany, S. M. K. K., 2009. *Optimisation of Influential Factors in Electrowinning of Tellurium by Means of PLS Modelling,* Lulea, Sweden: Lulea University of Technology.

Seborg, D. E., Edgar, T. F. & Mellichamp, D. A., 2004. *Process Dynamics and Control.* New Jersey: John Wiley & Sons, Inc.

Smith, L. I., 2002. *A tutorial on Principal Component Analysis.* [Online] Available at: http://www.cs.otago.ac.nz/cosc453/student_tutorials/principal_components.pdf

Tyroler, P. M., 1987. *Copper Electrowinning at Inco's Copper Refinery,* Copper Cliff, ON: Inco Ltd., Copper Refinery.

Vale Canada Ltd, 2014. *EW Short Description,* Copper Cliff, ON: Vale Canada Ltd..

Vale Ltd., 2012. *Copper Cliff Nickel Refinery Electrowinning Plant Copper Plating System,* Copper Cliff, ON: Vale Ltd. Ontario Operations.

Vale Ltd., 2012. *Copper Cliff Nickel Refinery Electrowinning Plant Selenium/Tellurium Removal System,* Copper Cliff, ON: Vale Ltd. Ontario Operations.

Venkatasubramanian, V., Rengaswamy, R., Yin, K. & Kavuri, S. N., 2003. A review of process fault detection and diagnosis Part I , II and III. *Computers & Chemical Engineering*, Volume 27, pp. 293-311, 313-326, 327-346.

Villegas, T., Fuente, M. J. & Rodriguez, M., 2010. *Principal component analysis for fault detection and diagnosis: experience with a pilot plant.* Wisconsin, 9th WSEAS international conference on computational intelligence, man-machine systems and cybernetics.

Wang, S., Wesstrom, B. & Fernandez, J., 2003. A Novel Process for Recovery of Te and Se from Copper Slimes Autoclave Leach Solution. *Journal of Minerals & Materials Characterization & Engineering, Vol.2,No.1,* pp. 53-64.

Wise, B. M. & Gallagher, N. B., 1996. The process chemometrics approach to process monitoring and fault detection. *Journal of Process Control,* Volume 6, pp. 329-348.

Yoon, S. & MacGregor, J. F., 2001. Fault diagnosis with multivariate statistical models part I: using steady state fault signatures. *Journal of Process Control,* Volume 11, pp. 387-400.

Zhang, J., 2006. Improved on-line process fault diagnosis through information fusion in multiple neural networks. *Computers & Chemical Engineering,* 30(3), pp. 558-571.